Simulating electronic excitation and dynamics with real-time propagation approach to TDDFT



Cite as: J. Chem. Phys. 155, 100901 (2021); doi: 10.1063/5.0057587 Submitted: 22 May 2021 • Accepted: 12 July 2021 • **Published Online: 8 September 2021**







Christopher Shepard, DRuiyi Zhou, Dillon C. Yost, Yi Yao, 3 and Yosuke Kanai Dellon C. Yost, Yi Yao, 3 and Yosuke Kanai Dellon C. Yost, Yi Yao, 13 and Yosuke Ya



- Department of Chemistry, University of North Carolina at Chapel Hill, Chapel Hill, North Carolina 27514, USA
- ² Department of Materials Science and Engineering, Massachusetts Institute of Technology, Cambridge, Massachusetts 02142, USA
- ³Thomas Lord Department of Mechanical Engineering and Materials Science, Duke University, Durham, North Carolina 27708, USA
- a) Author to whom correspondence should be addressed: ykanai@unc.edu

ABSTRACT

We give a perspective on simulating electronic excitation and dynamics using the real-time propagation approach to time-dependent density functional theory (RT-TDDFT) in the plane-wave pseudopotential formulation. RT-TDDFT is implemented in various numerical formalisms in recent years, and its practical application often dictates the most appropriate implementation of the theory. We discuss recent developments and challenges, emphasizing numerical aspects of studying real systems. Several applications of RT-TDDFT simulation are discussed to highlight how the approach is used to study interesting electronic excitation and dynamics phenomena in recent

Published under an exclusive license by AIP Publishing. https://doi.org/10.1063/5.0057587

I. INTRODUCTION

A majority of the electronic structure theory problems in quantum chemistry and condensed matter physics entail solving the timeindependent Schrödinger equation approximately for fermionic systems. At the same time, various properties of matter derive from the non-equilibrium condition on the Hamiltonian, and the timeevolution of the quantum state needs to be obtained by solving the time-dependent Schrödinger equation. External stimuli, such as an electromagnetic field, enter through time-dependent electronic Hamiltonian, and dynamical responses to the perturbation are encoded in the time-evolution of the quantum state (i.e., wavefunction, electron density, and density matrix). Starting with the time-dependent Hartree-Fock method in the late 1970s and the early 1980s, various theoretical methodologies, including correlated wavefunction methods,² have been developed for studying non-equilibrium response properties with the real-time propagation approach. Readers are referred to the comprehensive review by

Li et al. on the real-time propagation approach to time-dependent electronic structure theories in general.³ In the last decade, the real-time propagation approach to time-dependent density functional theory (TDDFT)⁴ has gained great popularity as a particularly practical methodology for studying the non-equilibrium response of real matters. The appealing balance between the accuracy and efficiency, together with its rigorous formal foundation based on the Hohenberg-Kohn theorem, has made density functional theory (DFT) calculation the most widely used computational approach for calculating various properties of matter from first principles. At the same time, its application is formally limited to ground-state properties, and many physical, chemical, and biological processes of interest in modern science and technology are concerned with dynamical behavior of electrons. Electron dynamics are at the heart of various non-equilibrium processes, including photo-excitation, hot carrier relaxation, charge recombination, and electronic stopping. Time-dependent density functional theory (TDDFT) based on the Runge–Gross theorem⁵ offers a powerful extension to the theory for studying these dynamical phenomena. 6-10 Through its formulation for the linear response regime in the frequency domain, 11-13 the TDDFT approach has become extremely popular for studying optical excitation of molecules and materials. 14 In this Perspective, we instead focus on the real-time propagation approach to TDDFT (RT-TDDFT),4 discussing recent development and challenges within the plane-wave pseudopotential (PW-PP) formulation in particular. 15,16 Since some of the first uses of the real-time propagation approach in the 1990s by Yabana and Bertsch, 4,17 RT-TDDFT has gained great popularity in various areas of chemistry and condensed matter physics. 18-24 RT-TDDFT can be used to model both linear and nonlinear responses to perturbations of various kinds and strengths. For large systems and certain regime of electronic excitation, RT-TDDFT can be computationally more efficient than the commonly used linear response TDDFT method even for calculating optical absorption spectra.²⁵ In recent years, there has been a surge in applications of RT-TDDFT to a wide range of excited state phenomena, such as interfacial charge transfer,²⁶, electronic stopping,^{28–38} optical absorption,^{17,18,39–41} core electron excitations, 34,42-45 electronic circular dichroism spectra, 46 exciton dynamics in nanostructures, 47,48 atom-cluster collisions, 49,50 high harmonic generation,^{51,52} laser-induced water splitting,⁵³ and topological quantum matter.54-57 The promulgation of RT-TDDFT as a means for simulating dynamic phenomena has led to its implementation in a variety of electronic structure codes, including NWChem, 18,58 SIESTA, 59,60 CP2K, 61,62 SALMON, 63 Octopus, 64, Q-Chem,⁶⁶⁻⁶⁸ GAUSSIAN,^{22,69} MOLGW,^{70,71} and Qbox/Qb@ll.^{72,16} Numerical details of the implementation vary widely among these codes, especially in the underlying basis sets used. While they all fall under the umbrella of RT-TDDFT, the numerical implementation is fundamental not only for the code developers but also for those who wish to apply the RT-TDDFT methodology to study various dynamical phenomena. The type of the phenomena under investigation can often dictate the most appropriate implementation of the theory in practice. In this perspective, we focus on the plane-wave pseudopotential (PW-PP) formulation of RT-TDDFT, discussing some recent advances and challenges in simulating electronic excitation and dynamics.

II. REAL-TIME PROPAGATION APPROACH TO TIME-DEPENDENT DENSITY FUNCTIONAL THEORY

TDDFT is based on the one-to-one correspondence between the time-dependent one-particle density and the time-dependent external potential. This correspondence is formally established by the Runge–Gross theorem,⁵ which extends the Hohenberg–Kohn theorem to the time-dependent case. There are several notable assumptions in the proof, such as the Taylor-expandable potential, and the validity of these assumptions is often not tested in practical applications of the theory. We refer to the textbook by Ullrich for excellent discussion of these aspects of TDDFT as a formal theory. We here focus on the practical side of numerical implementation and application as a theoretical method for investigating physical properties. While many time-independent problems in electronic structure theory can be cast as some form of an eigenvalue problem, RT-TDDFT entails to solving a set of coupled non-linear partial differential equations. At the heart of RT-TDDFT, the time-dependent

Kohn-Sham (TD-KS) equation reads

$$i\hbar \frac{d}{dt} |\phi_i(t)\rangle = \left\{ -\frac{\hbar^2}{2m_e} \nabla_{\mathbf{r}}^2 + \hat{v}_{ext}(\mathbf{r}, t) + \int d\mathbf{r}' \frac{\rho(\mathbf{r}', t)}{|\mathbf{r} - \mathbf{r}'|} + \hat{v}_{XC}(\mathbf{r}, t) \frac{\hbar^2}{2m_e} \right\} |\phi_i(t)\rangle, \tag{1}$$

where ϕ_i (\mathbf{r} , t) is the time-dependent single-particle Kohn–Sham wavefunction and ρ is the electron density. The $\hat{v}_{ext}(t)$ term accounts for all external potentials acting on electrons, such as those due to atom nuclei and applied external field, and \hat{v}_{XC} is the exchange–correlation (XC) potential. For simplicity, we assume that there is no XC vector potential in the Hamiltonian as one would have in time-dependent current-DFT. This differential equation looks as if it is a time-dependent Schrödinger equation. However, additional numerical complexity arises because the electron density (and often also the approximated XC potential) depends on the time-dependent KS wavefunctions themselves as

$$\rho(\mathbf{r},t) = \sum_{i}^{Occ.} |\phi_i(\mathbf{r},t)|^2.$$
 (2)

The dependence of the Hartree (electrostatic) and XC potential terms on the electron density (thus on the TD-KS wavefunctions) makes these coupled differential equations non-linear. Simply put, RT-TDDFT simulation amounts to, for a given initial state $\{\phi_i(\mathbf{r},t=0)\}_{i=1,\dots,N_{elec.}}$, numerically integrating the TD-KS wavefunctions in time according to the TD-KS equation [Eq. (1)]. Although it is mathematically a well-defined problem, accurate numerical integration of coupled non-linear differential equations is not a trivial task in general, as discussed in Sec. IV.

III. PLANE-WAVE PSEUDOPOTENTIAL FORMULATION

RT-TDDFT can be implemented in various different ways, most notably for expanding the TD-KS wavefunctions in various types of mathematical functions. In quantum chemistry, Gaussiantype orbital (GTO) functions have been widely used as the basis set functions, and Li et al. formulated the RT-TDDFT using GTOs. 69,74 At the same time, other numerical representations of the TD-KS wavefunctions are certainly possible and even more convenient in some situations. Historically, the implementation based on realspace grids has become popular for RT-TDDFT due to the original work by Yabana and Bertsch in 1996, 4,17 and the widely popular implementation in the Octopus code^{64,65} is based on the realspace grids. Our own RT-TDDFT method development in the Qbox/Qb@ll code, 72,16 on the other hand, is based on representing TD-KS wavefunctions using a set of plane-waves as the basis set, together with pseudopotentials that are designed to reproduce effects of core electrons around nuclei. 16,15 This so-called plane-wave pseudopotential (PW-PP) formulation^{75,76} is particularly convenient for studying extended systems, such as semiconductor solids and liquids,⁷⁷ and it has been traditionally more popular in condensed matter physics than in quantum chemistry. In addition to the fact that the plane-wave (PW) basis set is inherently compatible with the periodic boundary conditions (PBC) needed for studying extended systems, the PW-PP formulation is also convenient for performing the

Ehrenfest dynamics based on the atomic forces from RT-TDDFT. Because PWs are independent of the atom positions, the approach does not require additional effort to deal with the Pulay force as required when basis set functions depend on atomic positions. It is also free of the so-called egg-box effect, which refers to the break-down of translational invariance when using the real-space grids. At the same time, the PW-PP formulation generally requires a much larger number of basis set functions than what is typically required when using GTOs, and it is not uncommon for a PW-PP calculation to include millions of plane-wave coefficients. Having such a large Hilbert space requires a careful consideration when designing a parallelization scheme (e.g., MPI/openMP) and adapting certain numerical algorithms for operations such as matrix diagonalization and time integration.⁷⁵

Here, we briefly summarize the PW-PP formulation for a concise discussion of the rest of this Perspective. The Brillouin zone (BZ) integration is often important in modeling extended systems, and thus, the index i in Eq. (1) becomes a composite index that consists of both the momentum vector in the first BZ and the state index. According to the Bloch theorem, one can write the TD-KS wavefunctions in the form of Bloch states,

$$\phi_i(\mathbf{r},t) = \phi_{n,\mathbf{k}}(\mathbf{r},t) = \frac{1}{\sqrt{\Omega}} e^{i\mathbf{k}\cdot\mathbf{r}} u_{n,\mathbf{k}}(\mathbf{r},t), \tag{3}$$

where Ω is the volume of the simulation cell and $u_{n,k}$ is the periodic part of the Bloch state. In terms of plane-waves, one writes

$$\phi_{n,\mathbf{k}}(\mathbf{r},t) = \frac{1}{\sqrt{\Omega}} \sum_{\mathbf{G}} C_{n,\mathbf{k},\mathbf{G}}(t) e^{i(\mathbf{k}+\mathbf{G})\cdot\mathbf{r}},$$
 (4)

where the number of plane-waves in the simulation (super-) cell is determined by the kinetic energy cutoff such that $\hbar^2 |\mathbf{G}|^2 / (2m_e)$ < E^{cut}. The plane-waves do not depend explicitly on the positions of atomic nuclei, and they are present in the vacuum region outside of the immediate vicinity of molecules and material surfaces. This feature is particularly convenient for simulating high-energy electronic excitations and electronic stopping excitations as discussed later. Unfortunately, the number of plane-waves required for accurately representing spatially localized electrons, such as core electrons, is too large for many practical calculations, and the PW basis set is usually used with non-local pseudopotentials that are designed to replicate the interaction with missing core electrons near the atomic nuclei. 76,79-81 The pseudopotentials are obtained by inverting the atomic Kohn-Sham equation for a specific XC approximation, and the procedure is not unique and there exist several different schemes in the literature.⁸² Alternatively, planewave-based RT-TDDFT can also be implemented in the related framework of the projector augmented wave (PAW) method⁸³ instead of using the conventional pseudopotentials. The PAW method generally allows calculations to be converged with a smaller number of plane-waves. While the core electrons are frozen with respect to the environment, this approach enables reconstruction of all-electron wavefunctions through the PAW transformation operator. In the context of RT-TDDFT, it is worthwhile to note that the PAW transformation operator introduces the atomic position dependence, and the computation of energy-conserving force can be more involved for accurately performing Ehrenfest dynamics, as discussed by Ojanperä et al.84

The plane-wave formulations employ the Fast Fourier Transform (FFT) extensively as many key terms, such as the kinetic energy, are most conveniently evaluated in the reciprocal space. The computational cost of the FFT scales as $O(N_n N_{pw} \log N_{pw})$, where N_n is the number of Kohn-Sham states and N_{pw} is the number of planewaves in the basis set. The FFT and the orbital orthogonalization, which scales as O(N_n²N_{pw}), are generally the two most computationally expensive parts of calculations. While the orthogonalization procedure is necessary in solving for Kohn-Sham eigenstates, RT-TDDFT simulation does not require an explicit orthogonalization among the TD-KS wavefunctions at each time integration step as discussed below. Given the depth and the long history of the topic, readers are referred to Refs. 75 and 77 for detailed discussion. The PW-PP formulation was first adapted for RT-TDDFT by Sugino and Miyamoto,85 and it is particularly appealing for studying extended systems such as crystalline GaAs as done in their early work.86

IV. NUMERICAL INTEGRATION OF TD-KS EQUATIONS

Given the TD-KS equation [Eq. (1)], the time-evolution of the TD-KS wavefunctions can be written in the integral form as

$$\left\{ \left| \phi_i(t) \right\rangle = \widehat{U}(t, t_0) \left| \phi_i(t_0) \right\rangle \right\}_{i=1, \dots, N_{ol}}, \tag{5}$$

where the propagation operator is

$$\widehat{U}(t,t_{0}) = \widehat{1} + \sum_{n=0}^{\infty} \frac{1}{n!} \left(-\frac{i}{\hbar} \right)^{n} \int_{t_{0}}^{t} dt_{1} \int_{t_{0}}^{t} dt_{2} \dots \int_{t_{0}}^{t} dt_{n} \mathcal{T} \Big[\widehat{H}_{KS}(t_{1}) \widehat{H}_{KS}(t_{2}) \dots \widehat{H}_{KS}(t_{n}) \Big],$$
(6)

where $\mathcal T$ is the time-ordering operator and \widehat{H}_{KS} is the Kohn–Sham (KS) Hamiltonian, which constitutes the curly brackets in the righthand side of Eq. (1). Note that the Hamiltonians at different times do not commute in general. A stationary solution can be obtained in certain situations such as for a periodically driven Hamiltonian (i.e., a Floquet system) via construction of an effective Hamiltonian. However, the Hamiltonian's dependence on the electron density and the initial state complicates applying well-established analytical formalisms. Maitra and Burke discussed subtle impediments, for example, in extending the Floquet theory to TDDFT in Ref. 87. For general cases, the propagation operator [Eq. (6)] needs to be approximated with a sequence of many propagation steps with a much smaller dt, making numerical implementation/simulation essential for the real-time propagation approach in TDDFT. The integration time step dt depends on a number of factors, including the numerical integrator itself, basis set type, and the system/phenomena under investigation. A step size on the order of one atto-second is typically needed for a numerically stable and accurate integration of the TD-KS equations. As for any application of non-linear differential equations, numerical integration of the TD-KS equations also requires close attention to their stiffness. The stability of the numerical integrators becomes a major issue in practice because of the non-linearity in the KS Hamiltonian unlike for a time-dependent Schrödinger equation. 88-91 Both explicit methods, such as the fourth order Runge-Kutta, 15 and implicit methods, such as Crank-Nicolson⁹² and Enforced Time-Reversal Symmetry

(ETRS), 88,93 have been successfully employed in the PW-PP formulation. Using an explicit integrator, the TD-KS wavefunctions at the next time step are obtained as an explicit function of those at the current and previous time steps. For implicit integrators, the TD-KS wavefunctions at the next time step need to be obtained as solutions to a system of non-linear equations that are expressed in terms of the TD-KS wavefunctions at the current and the next time steps. This requires employing an iterative solution procedure or introducing controllable approximations so that a linear system is solved instead. Implicit methods usually involve more mathematical operations, but they are numerically more stable for solving stiff differential equations, allowing for a larger time step. The symplectic property of some implicit integrators is also discussed as being central to the simulation stability at long times.⁸⁹ In the PW-PP formulation, having the non-local pseudopotential term makes the evaluation of the exponential of the KS Hamiltonian more complicated if required as in some integration methods.85 In general, many appear to concur that no single integrator is perfect for simulating all phenomena and systems. The most suitable integrator depends not only on the type of problems to study but also on the basis set type (e.g., plane-waves vs Gaussians) used to represent the TD-KS wavefunctions as well as other computational considerations. Having a larger time step does not necessarily mean that an implicit integrator is always a better choice in practice because the computation time to perform each integration step might be significantly more, and actual implementations of implicit integrators are also often dependent on the performance of the linear solver. The scaling of integration methods with respect to the number of processors in massively parallel high-performance computers (HPC) is another practical consideration for large-scale RT-TDDFT applications. Numerical methods for solving non-linear differential equations continue to remain a very active area of research with great impacts on various fields, including RT-TDDFT simulation.

V. EXCHANGE-CORRELATION APPROXIMATION

As the electron dynamics simulated are dependent on the exchange-correlation (XC) potential, the importance of XC approximation cannot be overstated.⁹⁴ In TDDFT, approximations to the XC potential arise through two different aspects: The first is on the usual spatial dependence on the electron density, as in the case of the ground-state DFT. The second is the history dependence, or the memory, of the XC effect on the electron density from earlier times. Here, we do not consider time-dependent *current*-density functional theory (TDCDFT), which formally extends the theory to the oneto-one mapping between the vector potential and the current density, giving rise to the exchange-correlation vector potential. The Runge–Gross⁵ and van Leeuwen theorems^{5,100} prove the unique existence of the time-dependent XC potential, $v_{XC}[\rho, \Psi(t_0)](\mathbf{r}, t)$. In principle, the exact XC potential at time t is functionally dependent on the density $\rho(\mathbf{r}, t' < t)$ as well as on the initial many-body state at $t = 0, \Psi(t_0)$. As can be imagined, its exact form is extremely complicated. To make the theory practical for studying real systems, one often employs the adiabatic approximation, which entails neglecting the electron density history and the dependence of the initial manybody state. 101 Therefore, often in practice, the XC potential depends only on the instantaneous electron density (or TD-KS wavefunctions) at the time t. Adapting the adiabatic approximation is

convenient for practical RT-TDDFT simulation also because the total electronic energy then becomes a constant of motion.¹⁵ By expressing the energy functional as

$$E[\rho(\mathbf{r};t)] = \sum_{i} \left\langle \phi_{i}(t) | -\frac{\hbar^{2}}{2m_{e}} \nabla_{\mathbf{r}}^{2} | \phi_{i}(t) \right\rangle + \int \rho(\mathbf{r},t) \widehat{V}_{ext}(\mathbf{r},t) d\mathbf{r}$$

$$+ E_{H}[\rho(\mathbf{r};t)] + E_{XC}(t), \qquad (7)$$

the time-dependence of the electronic energy is

$$\frac{d}{dt}E = \sum_{i} \left\{ \left| \phi_{i}(t) | \widehat{H}_{KS}[\rho(t)] | \frac{d}{dt} \phi_{i}(t) \right| + c.c. \right\}
+ \int \rho(\mathbf{r}, t) \frac{\partial}{\partial t} \widehat{v}_{ext}(\mathbf{r}, t) d\mathbf{r}.$$
(8)

When the external potential does not change in time (i.e., no atomic movements or time-dependent perturbating field), the right-hand side of Eq. (8) vanishes as long as the adiabatic approximation is adapted for the XC potential. 15 Having such physical quantities, such as the energy as a constant of motion, is convenient for assessing the quality of numerical integration, and it is also essential in some applications, such as studying electronic stopping as discussed in Sec. VI C. Although essentially all practical RT-TDDFT simulations of real systems adapt this adiabatic approximation today, it is known to fail in some exactly solvable models. 102-104 The TDCDFT approach with the XC vector potential is likely to have a better chance of capturing XC effects beyond the adiabatic approximation.⁹⁴ At the same time, some recent works report notable successes with incorporating memory effects in the XC potential for model systems by employing machine-learning techniques such as the artificial neural network. 105 The development of better approximations to the XC potential via machine-learning techniques is an area of exciting future growth in general (see, for example, Ref. 106).

Many outstanding challenges remain for the XC functional development, especially for the PW-PP formulation, even when the adiabatic approximation is satisfactory. Compared to the DFT/TDDFT implementation based on localized basis set functions such as GTOs, the itinerant character of the plane-wave basis set has made the PW-PP formulation lag behind in adapting more sophisticated XC approximations beyond the generalized gradient approximation (GGA). Only in the last decade, meta-GGA and hybrid XC functionals have become more widely adapted in the context of ground-state DFT and also in first-principles molecular dynamics (FPMD) simulations. 107-112 Specifically, for hybrid XC approximations with the exact Fock exchange, novel algorithmic innovations made it possible to calculate the exchange integral efficiently using the plane-waves as the basis set functions. 109,113-116 Although the PW-PP formulation still mostly employs the LDA and GGA XC approximations, efficient implementations of meta-GGA and hybrid XC approximations have become available also in the context of RT-TDDFT in the last few years, 34,117 thanks to new algorithmic developments.^{54,114,118} This is a particularly welcome development since simulations involving long-range charge transfer are likely to benefit from hybrid and some meta-GGA XC approximations¹¹⁹ that better remedy the self-interaction/delocalization error.¹²⁰

VI. RECENT DEVELOPMENT AND PERSPECTIVE

A. Gauge invariance

Gauge invariance is often exploited in two different manners for RT-TDDFT. First, the gauge freedom exists for transforming the time-dependent KS wavefunctions as their unitary transformation preserves the time-dependent electron density. Secondarily, the gauge invariance in classical electrodynamics is widely exploited in modeling of extended systems; the gauge freedom between the scalar potential and vector potential is used for incorporating the electromagnetic field in the Hamiltonian. The gauge invariance of the TD-KS wavefunctions can be exploited in RT-TDDFT, as physical properties depend on the electron density but not on the individual TD-KS wavefunctions. Under arbitrary unitary transformations, the physical properties that derive from the electron dynamics are unchanged, but certain gauge transformations can be advantageous in some situations. Recently, several RT-TDDFT implementations have exploited this gauge freedom inherent in the TD-KS equations. For example, in a recent work by Lin and co-workers, the so-called parallel transport gauge was used to achieve a numerically efficient propagation for electron dynamics.¹¹⁸ In the parallel transport gauge, the unitary transformation is performed such that oscillations of the TD-KS wavefunctions are minimized. This allows for significantly larger integration time steps to be used with implicit time integration schemes, such as the Crank-Nicolson method. This provides a great computational advantage in practical RT-TDDFT simulations, especially when hybrid XC functionals are used. 114,117 In another work, Yost et al. employed the maximally localized Wannier function (MLWF)¹²¹ gauge for RT-TDDFT, as this gauge offers several advantages.⁵⁴ Due to the nearsightedness principle of electrons, 122,123 the MLWF orbitals can be made to highly localize in space for insulating systems with an energy gap (see Fig. 1, for instance), 121 and this spatial localization can be exploited in various ways.124

For example, this spatial localization can be exploited for efficient implementation of hybrid XC functionals by reducing the computational cost associated with the Fock exchange integrals, as done for FPMD¹²⁵ based on the MLWF orbitals. 126,127 The idea can be extended to RT-TDDFT using the time-dependent MLWFs (TD-MLWFs).⁵⁴ One can reduce the number of the exchange integrals that need to be evaluated due to the spatially localized nature of the TD-MLWFs, whereas TD-KS wavefunctions are generally itinerant in extended systems. Because a minimal spatial overlap is expected for those TD-MLWFs that are distant, one can possibly neglect some of the exchange integrals based on their geometric centers and spreads of the TD-MLWFs. Using a representative system of crystalline silicon (a 256-atom simulation cell) as an example, Fig. 2 shows how the computational cost and the numerical accuracy are affected by reducing the number of the exchange integrals as a function of the cutoff distance between a pair of TD-MLWFs, for the PBE0 hybrid XC^{128,129} approximation. The electronic energy is the key constant-of-motion for RT-TDDFT simulations as discussed above. Figure 2 shows that the computational cost can be reduced dramatically without sacrificing the simulation accuracy. The approach becomes even more appealing for simulation of increasingly larger systems. Even when a larger silicon simulation cell with 512 atoms is used, the Wannier functions can be localized to the same extent due to the nearsightedness principle. 122,123

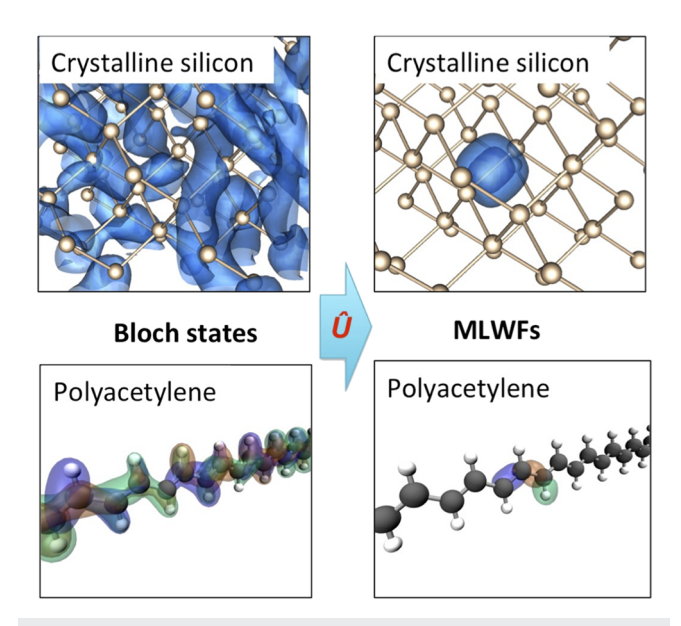


FIG. 1. Examples of the gauge transformation from the Bloch states to maximally localized Wannier functions (MLWFs) in crystalline silicon and polyacetylene. For silicon, isosurfaces of one representative Bloch state is shown, together with isosurfaces of one MLWF localized on a Si–Si bond. For polyacetylene, three Bloch states are shown, together with three MLWFs that are localized on CH (green), CC single (orange), and CC double (blue) bonds.

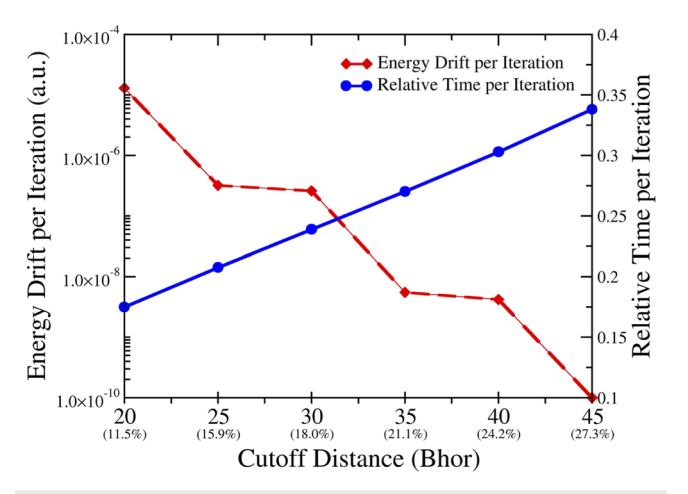


FIG. 2. Numerical accuracy and efficiency of employing a distance cutoff using TD-MLWFs for evaluation of Fock exchange integrals in the PBE0 hybrid XC approximation. Crystalline silicon is simulated using a 256-atom simulation cell with PBC. The percentage in the parentheses is for the number of the exchange integrals evaluated for the given cutoff distance. The PW cutoff energy of 25 Ry was used with PBE pseudopotentials of Hamann–Schlüter–Chiang–Vanderbilt (HSCV) type.^{80,130} An ETRS integrator was used with the integration time step of 0.05 a.u. The calculations were performed on 352 processors on eight Broadwell nodes (Intel Xeon E5-2699A v4 –2.4 GHz) of Dogwood cluster at the University of North Carolina at Chapel Hill. Only MPI (no open-MP/SIMD) was used for the test

TABLE I. The wall-clock time per iteration for simulating crystalline silicon using a larger 512-atom with PBC. The PBE-GGA values are included for comparison. The calculations were performed on 704 processors on 16 nodes using the same settings as in Fig. 2.

| | Cutoff distance (bohr) | Ex integrals evaluated (%) | Energy drift per iteration (a.u.) | Time per iteration (s) | Relative iteration time |
|------|---------------------------|----------------------------|-----------------------------------|------------------------|-------------------------|
| PBE | N/A | N/A | $<1.0 \times 10^{-10}$ | 19.9 | 0.009 |
| PBE0 | N/A | 100 | $<1.0 \times 10^{-10}$ | 2227.8 | 1 |
| PBE0 | 25 | 7.4 | 4.1×10^{-7} | 271.3 | 0.12 |
| PBE0 | 30 | 9.0 | 3.6×10^{-7} | 278.4 | 0.13 |

Thus, the same cutoff distance can be used and even larger fractions of the exchange integrals can be removed without degrading the accuracy, as shown in Table I. The computational cost of the PBE0 hybrid XC functional is typically about two orders of magnitude higher than that of the Perdew–Burke–Ernzerhof (PBE) GGA XC functional, but this TD-MLWF approach reduces the increased cost to be only one order of magnitude. A well-known limitation of semi-local XC functionals is its inability to describe long-range charge transfer accurately. Using the TD-MLWF gauge, the ability to employ range-separated hybrid XC approximations in RT-TDDFT is expected to greatly facilitate studies of charge transfer dynamics at heterogeneous systems, such as molecule–semiconductor interfaces.

The gauge invariance of the TD-KS wavefunctions has been used also to formulate the so-called dynamical transition orbitals (DTO) in order to obtain a particle-hole description within RT-TDDFT dynamics in a recent work by Zhou and Kanai. Motivated by the natural transition orbitals, 32 which are widely used in linear response TDDFT, the singular value decomposition of

time-dependent orbital transition matrices can be performed to obtain time-dependent particle/hole orbitals. Then, a new set of the gauge-invariant orbitals, dynamical transition orbitals (DTO), can be formulated as a linear combination of the hole and particle orbitals as

$$\left|\psi_{i}^{DTO}(t)\right\rangle = a_{i}(t)\left|\psi_{i}^{h}(t)\right\rangle + b_{i}(t)\left|\psi_{i}^{p}(t)\right\rangle,\tag{9}$$

where $|\psi_i^h(t)\rangle$ and $|\psi_i^p(t)\rangle$ are the hole and particle orbitals, respectively. The expansion coefficients satisfy

$$a_i(t) \ge 0$$
, $b_i(t) \ge 0$, $a_i(t)^2 + b_i(t)^2 = 1$. (10)

This gauge-invariant formulation is particularly appealing for developing a conceptual understanding of RT-TDDFT dynamics through the particle–hole transition description.

Figure 3 shows an example of crystalline silicon optically excited at 2.5 eV. Projecting onto the KS eigenstates (of the equi-

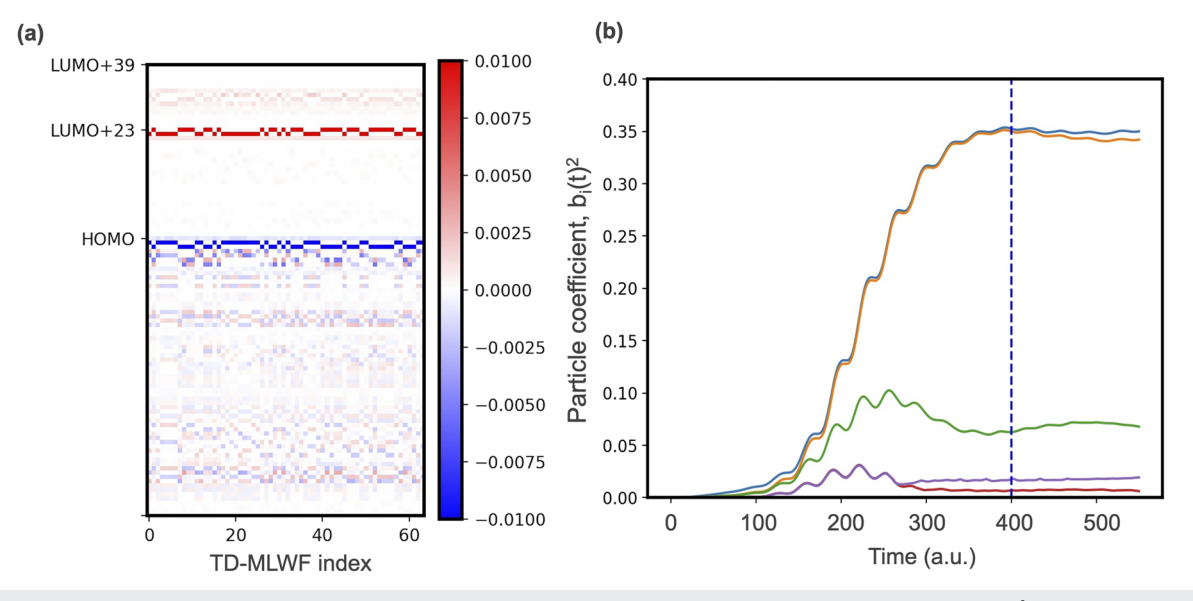


FIG. 3. (a) Changes in the projection matrix of TD-MLWFs onto KS eigenstates at t = 400 a.u. (b) Time-evolution of the particle coefficient, $b_i(t)^2$, for the dynamical transition orbitals with the five most dominant changes. To model the crystalline silicon optically excited at 2.5 eV, a 32-atom simulation cell elongated in the direction of optical pulse $(41.1 \times 10.3 \times 10.3 \text{ bohrs})$ was used. The LDA XC approximation was employed with the PW cutoff energy of 40 Ry and with HSCV pseudopotentials. A fourth-order Runge–Kutta integrator was used with an integration step size of 0.05 a.u.

librium system) reveals that all TD-MLWFs respond similarly to the optical excitation pulse as perhaps expected, and the electronic excitation is embodied in many single-particle transitions among the KS eigenstates [see Fig. 3(a)]. At the same time, the same electronic excitation can be described by changes in a much smaller number of the dynamical transition orbitals via the DTO unitary transformation [see Fig. 3(b)]. Here, single-particle transitions from the hole orbital to the particle orbital in few individual DTOs are able to describe the same electron dynamics responsible for the excitation. Such a compact particle—hole description of electronic excitation phenomena is likely to be of great value as RT-TDDFT simulations are applied to increasingly complex systems. The DTO approach has been already used to examine exotic electron transport such as those observed in topological quantum matter.⁵⁷

The gauge invariance of the electromagnetic field is a central concept in classical electrodynamics, and it is widely exploited in modeling of extended systems. Studies of the dynamical response of electrons to light is a very active research topic for RT-TDDFT simulations, and the external perturbation is usually modeled via a time-dependent electromagnetic field that is spatially homogeneous on the stimulated length scale. Formally, application of the Runge-Gross theorem cannot be rigorously justified when a homogeneous field acts on a periodic system due to a non-vanishing surface integral, instead requiring the TDCDFT formulation with an explicit dependence on the current density.¹³³ For isolated systems such as molecules, it is often convenient to model effects of the electromagnetic field on electrons through an additional scalar potential term in the KS Hamiltonian [i.e., $v(t) = e\mathbf{E}(t) \cdot \hat{\mathbf{r}}$] via the electric dipole approximation. While the PW-PP formulation is naturally suitable for modeling extended systems using the periodic boundary conditions (PBCs), the TD-KS wavefunctions are generally highly itinerant in the simulation cell, making the direct application of this so-called length-gauge approach incompatible. However, by transforming to the above-discussed spatially localized Wannier gauge, the operation of this scalar potential ^{134,135} on individual TD-MLWFs becomes well defined, making it possible to employ the length-gauge formulation as discussed in Ref. 54. Alternatively, the gauge freedom in classical electrodynamics allows us to describe the same field using a time-dependent vector potential term [i.e., $A(t) = -c \int_{-\infty}^{t} \mathbf{E}(t') dt'$] in the Hamiltonian. This formulation is usually referred to as the velocity-gauge approach, and it is widely used for studying extended systems with PBC. We note, however, that having non-local pseudopotentials in the KS Hamiltonian as we do in the PW-PP formulation rather complicates the gauge-invariance principle of electrodynamics, 136 as discussed by Ismail-Beigi et al., 137 and an approximated form is usually used in practice. Despite some formal and practical limitations, recent studies have shown that many response properties can be acquired reliably. For instance, Pemmaraju et al. 43 and Noda et al. 63 implemented the velocity-gauge formulation in RT-TDDFT, and various optical response properties of crystalline silicon have been successfully calculated.

B. Massively parallel computation

RT-TDDFT simulation relies not only on methodological advancement for the implementation of the theory but also on software engineering. In particular, taking advantage of modern high-performance computers (HPCs) has become essential for

electronic structure calculations of complex systems in the last few decades. Tremendous computing resources have become available in the form of massively parallel computers with millions of computing cores working simultaneously in parallel. Massively parallel computation is an important aspect of modern software engineering for many electronic structure codes. Dynamical simulations, such as FPMD and RT-TDDFT, tend to be particularly demanding computationally, and massively parallel computation on modern HPCs is essential for studying large extended systems. Our own RT-TDDFT development has indeed focused on performing complex simulations by exploiting massively parallel HPCs. 16,93 The use of planewaves as the basis set functions naturally caters to the massively parallel implementation because the large number of the planewave coefficients can be distributed effectively across compute nodes and also due to the availability of efficient MPI-enabled FFT subroutines. Our RT-TDDFT development in the Qb@ll⁷³ branch of the Qbox code^{72,138} takes advantage of several parallelization strategies (i.e., MPI/Open-MP/SIMD), as discussed in Refs. 16 and 93. The RT-TDDFT simulation can be made to scale efficiently on a very large number of processors on different HPC hardware architectures, as shown in Fig. 4 (a strong scaling test for crystalline gold with 27 200 electrons); the code, for instance, is able to efficiently utilize over one million processor cores in an IBM Blue Gene/Q machine, Sequoia at Lawrence Livermore National Laboratory. Unlike for the ground-state FPMD methods, RT-TDDFT simulation does not require a separate wavefunction orthogonalization procedure at each time step, and this property makes RT-TDDFT naturally amenable to a greater scaling. Andrade et al. indeed have exploited this feature for performing efficient FPMD simulation within the Ehrenfest dynamics formalism. 139 Nevertheless, achieving great performance on massively parallel HPCs requires significant optimization efforts on communication and kernels for the specific hardware architecture as demonstrated for the IBM Blue Gene/O machine.⁹³ In coming decades, the use of Graphics Processing Unit (GPU) coprocessors along with central

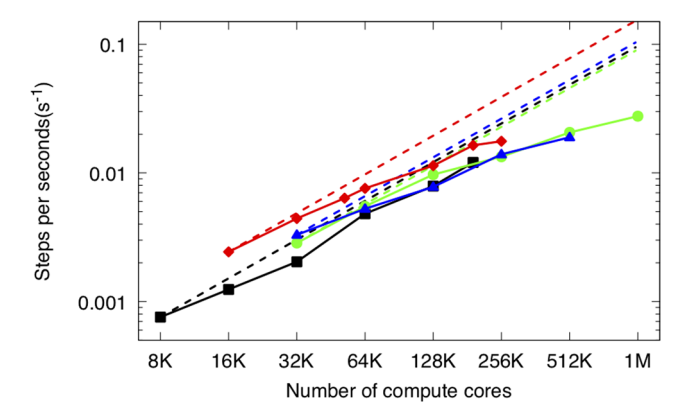


FIG. 4. Strong scaling test of RT-TDDFT implementation in the Qbox/Qb@ll code using the ETRS integrator with LDA XC approximation over a large number of processor cores. The simulation cell for this crystalline gold contains 1600 atoms (27 200 electrons). The scaling tests were performed on the IBM Blue Gene/Q Sequoia (green) and Mira (blue), Cray XE6 Blue Waters (red), and Cray XC40-Intel KNL Theta (black).

processing unit (CPU) processor cores is likely to become important in HPCs. Several operations, such as FFT, can take advantage of efficient GPU computation. Despite significant hardware-related challenges, an effort for achieving great efficiency in utilizing GPU coprocessors is already under way. 140

C. Applications

We discuss here several applications of the RT-TDDFT simulation, focusing on those that highlight particular strengths of the plane-wave pseudopotential (PW-PP) formulation.

1. Optical excitation in dense manifold

TDDFT is widely employed within the linear response theory framework¹² for computing optical absorption spectrum, often via Casida's equation.¹¹ The RT-TDDFT method is equally applicable, and it has been employed successfully in various studies of optical excitation.3 The PW-PP formulation is particularly suitable for optical absorption spectrum calculation of condensed matter systems and of high-energy excitation. For the absorption spectrum calculation, one must choose an appropriate "excitation" procedure that simultaneously excites the system in a superposition of its eigenstates. Any perturbation that is suddenly "switched on/off" at the next time step has the effect of inducing electronic oscillations that includes all frequency components and thus results in a broadband excitation of the system (i.e., δ -kick). The conventional linear response TDDFT approach becomes computationally very expensive when a dense manifold of many excited states is responsible for the absorption spectrum such as those of condensed matter systems and of higher-energy excitation. The computational cost of RT-TDDFT, on the other hand, does not increase with the number of excited states involved. Only the occupied TD-KS wavefunctions need to be propagated in time explicitly in response to the perturbating field.

For condensed matter systems, the imaginary part of the dielectric function is directly related to the optical absorption, whereas the real part is related to dispersion. The dielectric function can be obtained from computing an isotropic average of the frequency-dependent conductivity as

$$\varepsilon(\omega) = 1 + \frac{4\pi i}{3\omega} Tr[\sigma_{\mu\nu}(\omega)], \tag{11}$$

where $\sigma_{\mu\nu}(\omega)$ is the complex conductivity tensor. The conductivity tensor can be obtained straightforwardly by Fourier transforming the time-dependent current. As an example, Fig. 5 shows the optical absorption spectrum of liquid water. In order to take into account dynamical effects of nuclei at room temperature, four snapshots are taken from the FPMD simulation. In the MLWF gauge, the TD-MLWFs are spatially localized as lone-pair electrons and OH bonding electrons on individual water molecules, and molecular-level insights can be obtained by analyzing the absorption spectrum in terms of their contributions. As can be seen in Fig. 5, the lone-pair electrons are primarily responsible for the prominent excitation peak below 20 eV. Such spatial decomposition enables RT-TDDFT simulation to be used not only for prediction but also for gaining a molecular-level understanding of the experimental spectrum of complex heterogeneous systems.

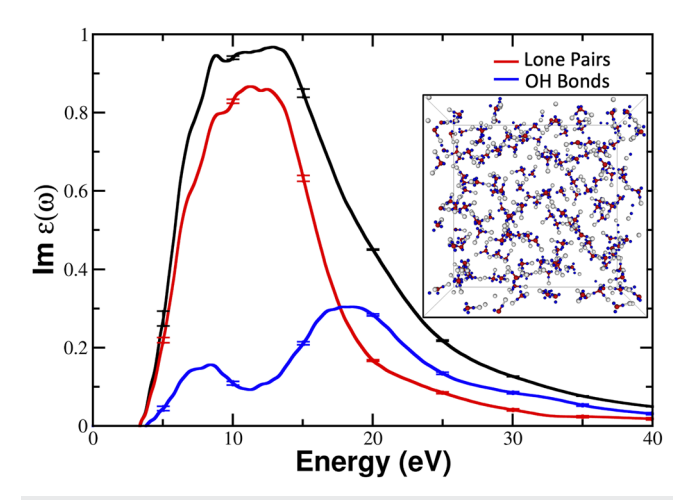


FIG. 5. Imaginary part of the dielectric function for liquid water at room temperature. The error bar indicates the statistical uncertainty from averaging the spectra over four snapshots of FPMD simulation. The simulation cell contains 162 molecules with PBC. Geometric centers of TD-MLWFs are shown in the inset, and they can be identified as the lone-pair electrons and OH bonds on individual molecules. Their contributions to the spectrum are also shown. The simulation was performed with the ETRS integrator with the step size of 0.05 a.u., with the PBE128 GGA XC approximation with HSCV pseudopotentials. The PW cutoff energy of 50 Ry was used. δ-kick electric field perturbation was used to excite the system at t=0.

In addition to simulating extended systems with the periodic boundary conditions (PBCs), calculation of high-energy optical excitation is also particularly suitable for the PW-PP formulation. For high-energy excitation, the excited electron density tends to extend into the vacuum region, requiring basis set functions away from atomic nuclei, and thus the use of plane-waves as the basis set functions is particularly convenient. At the same time, the PBC are automatically imposed, and the convergence of the simulation cell size needs to be checked so that artificial interactions among the periodic images do not affect computed properties. For isolated molecules, the optical absorption spectrum is usually given in terms of the dipole strength function,

$$S(\omega) = \frac{4\pi\omega}{3c} Tr[Im\sigma_{\mu\nu}(\omega)], \qquad (12)$$

where $\sigma_{\mu\nu}(\omega)$ is the polarizability tensor. Figure 6 shows the case of a single water molecule as an example and how the size of the cubic simulation cell (L³) affects the calculated optical absorption spectrum. As can be seen, the oscillations in the absorption spectrum using the small simulation cell (L = 15 bohrs) are an artifact, and they disappear when the simulation cell is made large enough (L = 100 bohrs). Although most ground-state properties would have converged even with the small simulation cell, some excited-state properties require more stringent convergence criteria. Figure 6 shows that RT-TDDFT simulation is able to model experimental features of the absorption spectrum over a wide range of the excitation energy over 100 eV, including the energy regime for which the ionization dominates the transition.

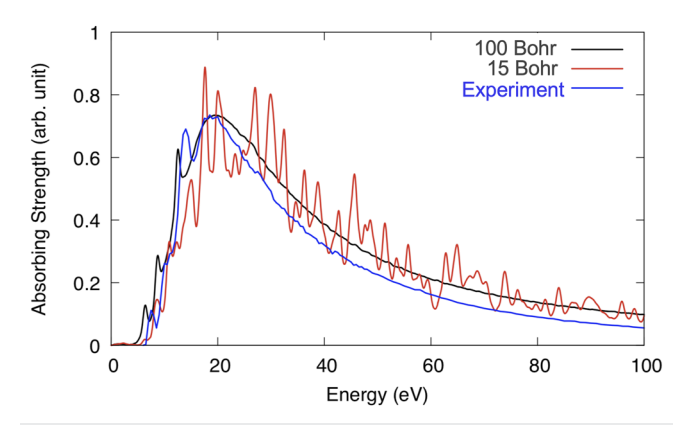


FIG. 6. Optical absorption spectrum of a single water molecule. The LDA XC approximation was used with the PW cutoff energy of 40 Ry and with HSCV pseudopotentials. δ -kick electric field perturbation was used to excite the system. The ETRS integrator was used with the time step size of 0.05 a.u. Experimental values are taken from Ref. 141.

2. Large-scale simulation of solvated DNA under proton irradiation

RT-TDDFT simulation is particularly amenable to massively parallel implementation as discussed earlier, and it enables us to investigate structurally complex systems using modern high-performance computers. Investigating how high-velocity protons induce electronic excitation in DNA solvated in water represents such a massively parallel simulation, as shown in Fig. 7. Developing a molecular-level understanding of this dynamical processes is important for ion beam cancer therapies, and the large-scale computation

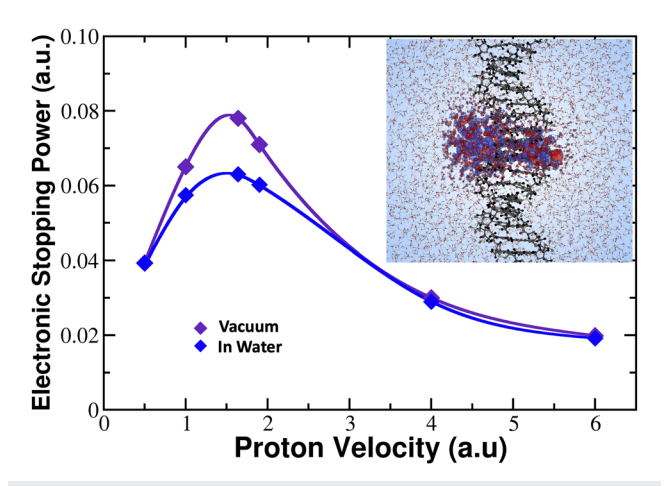


FIG. 7. Effects of water solvation on DNA electronic stopping power for the projectile/irradiating proton for a particular projectile proton path through the center of the DNA. The simulation was performed with the ETRS integrator with the step size of 0.0827 a.u., with the PBE GGA¹²⁸ XC approximation and with HSCV pseudopotentials. The PW cutoff energy of 50 Ry was used. The simulation cell contains ~13 000 explicit electrons (10 DNA base pairs along the Z direction with more than 1000 water molecules) with PBC, and it is shown in the inset.

allows us to employ first-principles electronic structure theory for helping solve important societal problems.

The simulated system contains ~13 000 electrons, and a total of up to 262 144 processor cores are used simultaneously on the Theta machine at the Argonne National Laboratory. In these simulations, the projectile proton (i.e., irradiating proton) initially moves through the water region and then through the DNA, inducing electronic excitation via energy transfer along the way. While such a large-scale RT-TDDFT simulation cannot be performed routinely today, the explicit quantum-mechanical treatment of solvent water molecules is needed here because some electrons are excited away from the DNA into the water region at some projectile proton velocities. In this so-called electronic stopping process, a particularly important quantity is the energy transfer rate from the projectile proton to electrons. This energy transfer rate is typically referred to as electronic stopping power, and it is given as in terms of the amount of the energy transferred per unit distance of the charged particle movement (i.e., projectile/irradiating proton here), and it is given as a function of the constant particle velocity. As discussed extensively in our work, ^{29,32,33} the electronic stopping power can be obtained by performing non-equilibrium RT-TDDFT simulations in which the irradiating projectile ion (e.g., proton) is moved at a constant velocity. In such non-equilibrium dynamics, the relevant constant of motion consists of the total electronic energy, E, and the work done by the projectile/irradiating ion, W_{ion} , ¹⁵ such that

$$\frac{d}{dt}E(t) + \frac{d}{dt}W_{ion}(t) = \frac{d}{dt}E(t) + \frac{d}{dt}\int \mathbf{F}_{ion}[\rho(t)] \cdot d\mathbf{R}_{ion}$$

$$= 0, \qquad (13)$$

where E is the quantum-mechanical electronic energy of the system [Eq. (8)] and \mathbf{F}_{ion} is the non-adiabatic force on the projectile ion. Given this energy conservation, the electronic stopping power can be obtained from the non-adiabatic force (sometimes called retarding force) on the projectile ion 142 or equivalently from the electronic energy increase in the non-equilibrium simulation. The geometrically averaged stopping power at a particular velocity, v, can be expressed as

$$S_{e}(\mathbf{v}) = -\left\langle \mathbf{F}_{ion}[\rho(t)] \cdot \dot{R}_{ion} \right\rangle_{\mathbf{v}}$$

$$= \left\langle \frac{dE[\rho(\mathbf{r};t)]}{d|\mathbf{R}|_{ion}} \right\rangle_{\mathbf{v}} = \left\langle \frac{dE[\rho(\mathbf{r};t)]}{dt} \right\rangle_{\mathbf{v}} \mathbf{v}^{-1}, \tag{14}$$

where the bracket indicates the geometrical ensemble average of the projectile ion trajectories. ^{16,32} In most instances, it is computationally more convenient to calculate the stopping power from the electronic energy increase because it typically converges faster than the force with respect to the basis set size. In Fig. 7, the stopping power is obtained as a function of the projectile proton velocity for one specific path that goes through the center of the DNA. Water solvation is found to decrease the stopping power of DNA under proton irradiation, particularly near the stopping power maximum, while the suppression of the energy transfer by the solvation is not observed for the higher proton velocities. The massively parallel implementation of RT-TDDFT enables us to take advantage of modern HPCs for studying the water solvation effect on DNA quantum-mechanically, allowing us to better model physiological conditions.

3. Exchange-correlation dependence of electronic stopping in the electron gas

Significant dependence of excitation energy on the XC approximation is widely appreciated already, and we illustrate its impact on the electronic stopping power. As a pedagogical example, we consider here the electronic stopping of protons in the uniform electron gas (i.e., jellium) in the Fermi fluid and Wigner crystal phases. The uniform electron gas is often employed to study different quantum phases of electrons because the balance between the electron-electron interaction and the kinetic energy can be modulated by changing the density. For the Fermi fluid phase of delocalized electrons (the high density regime), we use the Wigner-Seitz radius of $r_s = 2$ bohrs. Using approximate XC functionals in DFT, the Wigner crystal phase is obtained at $r_s = 70$ bohrs, which is lower than the best estimate from the diffusion quantum Monte Carlo calculation for the three-dimensional case ($r_s \sim 106$ bohrs). While there are differing philosophies on how the XC approximations should be developed, Perdew introduced the Jacob's ladder analogy of DFT, 144 advocating for developing more accurate approximations by satisfying more physical constraints through increasingly more complex dependence on the electron density and beyond. 145 In addition to the LDA, we employ here the PBE GGA approximation¹²⁸ and SCAN meta-GGA approximation. 146 They belong to the non-empirical formulation on the first three rungs of the DFT Jacob's ladder. Figure 8 shows that, for the Fermi fluid, all three XC approximations yield the same stopping power curve as a function of the proton velocity. Even with the increasingly complex dependency on the density gradient and the kinetic energy density (KED), both PBE GGA and SCAN meta-GGA functionals yield the same electronic stopping power for the Fermi fluid state as the LDA, as perhaps anticipated by their design. For comparison, Fig. 8 also shows the linear response theory result using the Lindhard dielectric function (for $r_s = 2$), which is perhaps the most widely used analytical model,³² together with the

widely used empirical SRIM model¹⁴⁷ based on experimental data on crystalline aluminum (which roughly corresponds to uniform electron gas with $r_s = 2$). The Wigner crystal phase represents, on the other hand, an opposing extreme in which the Coulomb repulsion among electrons dominates over the kinetic energy at low densities, and electrons become spatially localized. For the Wigner crystal, SCAN meta-GGA yields a stopping power curve that is noticeably different from those obtained using the LDA and PBE GGA functionals, providing an improved description for the electrons in this opposite limit. In the meta-GGA description, the kinetic energy density (KED) is used to distinguish between the single-orbital limit (i.e., von Weizacker KED) and the uniform gas limit (i.e., Thomas-Fermi KED), and it is likely responsible for the observed difference. The development of more accurate XC approximations will advance not only the excited state calculation but also the calculation of dynamical properties such as electronic stopping power in non-equilibrium RT-TDDFT simulation.

4. Non-adiabatic charge pumping in polymer

RT-TDDFT simulation has been used also to study novel non-adiabatic dynamics of electrons in topological systems. 54-57 Due to their unique connection to the Berry phase, Wannier functions are increasingly used in the investigation of topological materials. 148 As posited by Resta and Vanderbilt, 149 studying the behavior of Wannier centers can lead to developing molecular-level insights, especially valuable for real materials. The phenomenon of quantized topological pumps was first discussed by Thouless in 1983. 150 In recent years, different types of Thouless pumps have been demonstrated experimentally, 151,152 and Wannier functions can provide a physically intuitive description to understand the mechanisms of such a dynamic topological phenomenon. Most theoretical studies and descriptions of topological pumps assume complete

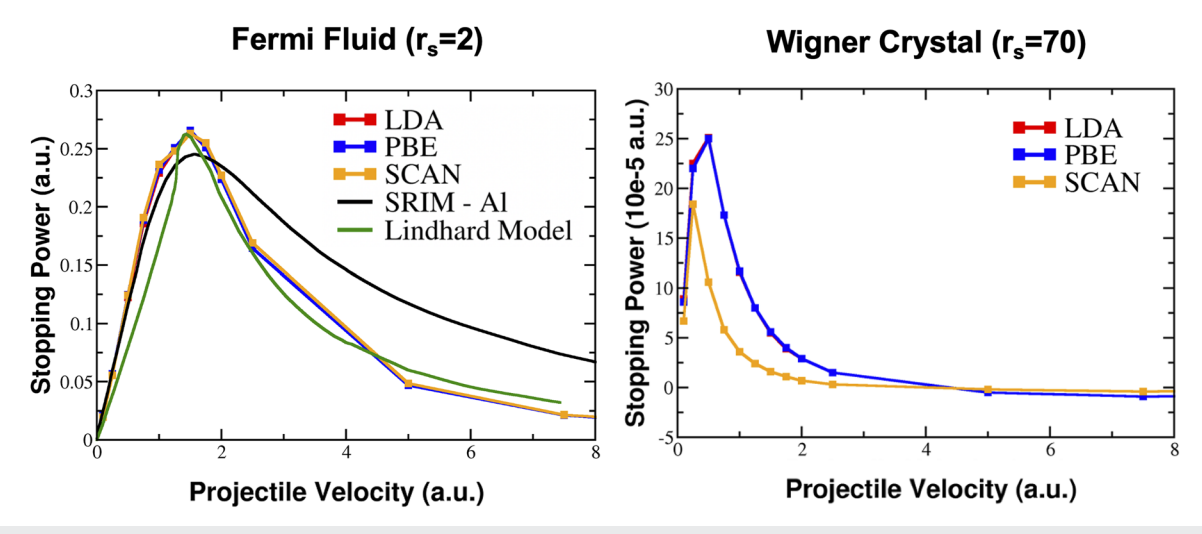


FIG. 8. Electronic stopping power of protons in the Fermi fluid and the Wigner crystal phases of the uniform electron gas. For the Fermi fluid, the simulation contains 466 electrons in the cubic cell with L=25 bohrs with the PW cutoff energy of 30 Ry. The Wigner crystal simulation employs one electron in the cubic cell with L=100 bohrs with the PW cutoff energy of 0.2 Ry. The ETRS integrator was used with 0.1 a.u. for the time step. For the Fermi fluid phase, the Lindhard model (with $r_s=2$) and SRIM model $r_s=100$ for bulk aluminum are shown for comparison.

adiabaticity of the Hamiltonian evolution while more recent work has begun to study non-adiabatic extension with a model system, such as the Rice–Mele Hamiltonian.¹⁵³ In our recent work, ^{54,57} we demonstrated using the time-dependent maximally localized Wannier function (TD-MLWF) gauge for studying the quantized transport beyond the adiabatic limit, in particular, to describe non-adiabatic Thouless pumping of electrons in *trans*-polyacetylene. The use of TD-MLWFs and also the DTO methodology enabled us to gain molecular-level insights into dynamic properties of the material characterized by topological invariants of the underlying electronic structure.⁵⁷

Building on the quantized charge transport behavior, one can envision a setup for an optically switchable transistor with the quantized current, as schematically shown in Fig. 9. In transpolyacetylene, the Peierls instability causes the carbon bonds to form alternating single/double carbon bonds, yielding the chiral (i.e., sublattice) symmetry in the Hamiltonian. Application of the static electric field along the polymer causes "tilting" of the periodic potential well, breaking the translation symmetry in the potential. The magnitude of this applied electric field is set small enough such that it polarizes the electronic system but no current flows (i.e., below dielectric breakdown threshold). The calculated optical absorption spectrum of this polymer shows a sharp peak at 2.8 eV,54 which corresponds to a resonant frequency of the double bonds (Fig. 9). A quasi-monochromatic optical pulse of the corresponding frequency can be then applied to drive a unidirectional quantized charge transport. Both the static and time-dependent external perturbing fields can be applied using the length gauge in the TD-MLWF gauge formulation, as discussed in Sec. VI A. Figure 10 shows the timeevolution of the geometric centers of double-bond TD-MLWFs

(which are simply referred to as the Wannier centers here) under several conditions, with the optical pulse ceasing at t~475 a.u. With the 2.8 eV optical pulse, the unidirectional current is induced but only when the static electric field is applied at the same time [see Figs. 10(a) and 10(b)]. Figure 10(b) shows that the Wannier center movement is not monotonically continuous but interestingly sharp transitions across the carbon atoms are observed. Without the static electric field, there is no current flow and the Wannier centers simply oscillate, even when the system is resonantly excited by the optical pulse at 2.8 eV. We find that no current is induced even with the static electric field unless the optical pulse is tuned to the specific resonance frequency. For instance, Figs. 10(c) and 10(d) show that the optical pulses at 1.4 and 5.6 eV do not result in electron transport. To summarize, the specific excitation frequency is necessary for the photoconductivity, and thus, the system can operate as an optically switchable transistor. The RT-TDDFT provides a powerful computational method to study various types of topological quantum materials beyond the usual adiabatic evolution limit as a first-principles approach and also in various environments, opening up exciting frontiers of research on topological systems.

D. Future outlook

In the last few decades, the real-time propagation approach to TDDFT, RT-TDDFT, has become a powerful computational approach for studying various optical excitation phenomena and non-equilibrium electron dynamics due to the appealing balance between the accuracy and computational efficiency of the DFT formalism. Studies of non-linear dynamics/effects in complex systems have significantly benefitted from the methodological development

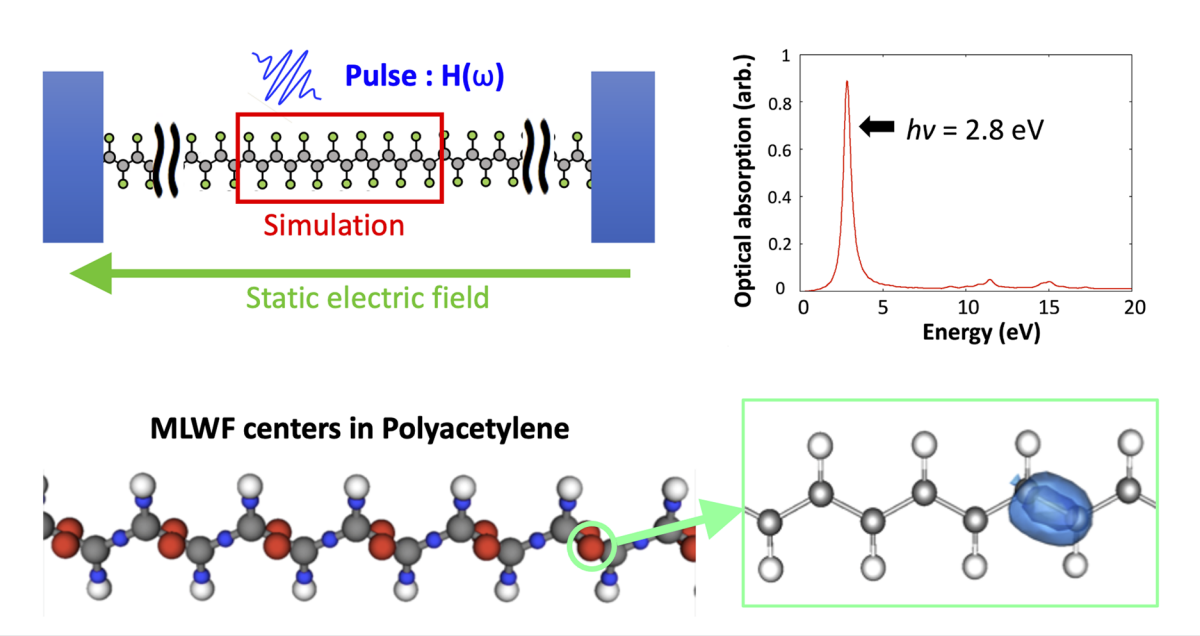


FIG. 9. Schematic of optically switchable transistor conceptual setup using a *trans*-polyacetylene between two electrodes. The simulation cell contains a 28-atom *trans*-polyacetylene chain with PBC ($34.28 \times 20.00 \times 20.00$ bohrs). The LDA XC approximation was employed, with the PW cutoff energy of 20 Ry, using HSCV pseudopotentials. The ETRS integrator was used with the time step of 0.1 a.u. The optical absorption spectrum of this 28-atom *trans*-polyacetylene shows a sharp excitation peak at hv = 2.8 eV. Geometric centers of MLWFs are shown for the equilibrium state, with red and blue spheres corresponding to double and single carbon–carbon bonds.

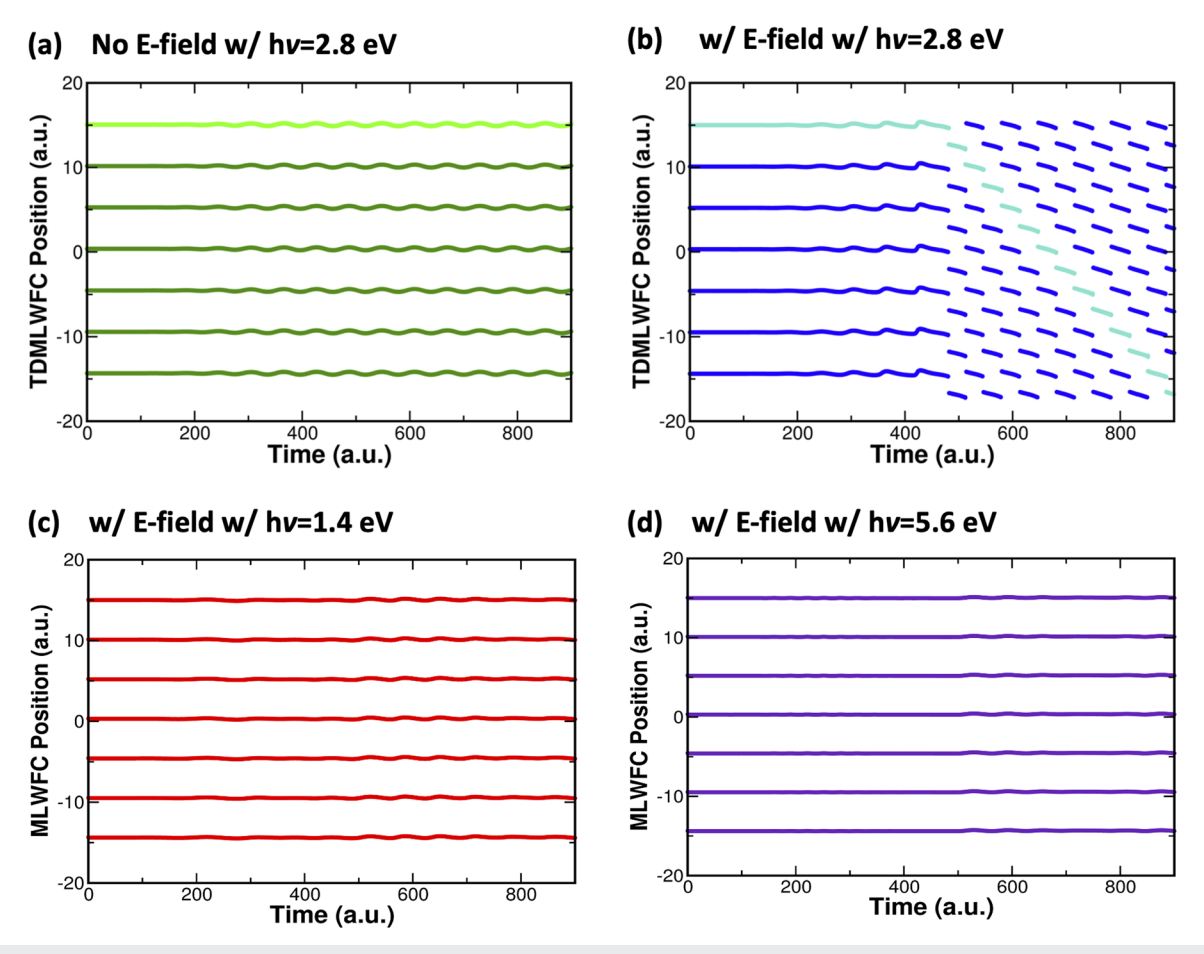


FIG. 10. (a) The movement of the geometric centers of the TD-MLWFs in response to the applied fields. The static electric field (E-field) is applied along the polymer chain with the field strength of 2.5×10^{-3} a.u. (b)–(d). Quasi-monochromatic optical pulse, enveloped in a Gaussian function with a full-width at half-maximum of 1.0 eV, was applied with the field strength of 1.0×10^{-3} a.u., with the optical frequencies of hv = 2.8, 1.4, and 5.6 eV.

with accompanied advancement of high-performance computing (HPC) technologies. Together with continued efforts on extending the exchange-correlation approximation for more sophisticated treatment of the many-body interaction, algorithmic innovations are also needed for efficient simulation of novel phenomena in increasingly complex systems. The plane-wave pseudopotential (PW-PP) formulation has benefited from many algorithmic innovations for incorporating increasingly sophisticated XC approximations in recent years, and RT-TDDFT simulation is poised to take advantage of such recent advances. Additionally, the importance of the numerical integrator cannot be overlooked in practical simulations. Stable and accurate numerical integration is at the heart of modeling dynamical phenomena, and our ability to access a longer timescale in RT-TDDFT simulation is fundamental for undertaking many applications. There are several important challenges that are specific to the PW-PP formulation of RT-TDDFT. While the PW-PP formulation is particularly convenient for studying extended systems and some phenomena, such as high-energy excitation, core electrons are replaced by non-local pseudopotentials, and dynamics

of core electrons are inherently neglected. Some recent advancement in the pseudopotential theory allows us to include core electrons as we have shown in Ref. 34. However, the computational cost increases dramatically if core electrons are to be modeled accurately. RT-TDDFT has been extended to include relativistic effects via four/two-component Dirac methods in recent years, 154,155 and the treatment of core electron dynamics is likely a significant methodological challenge for the PP-PW formulation. The use of nonlocal pseudopotentials is another aspect that has not been fully explored in RT-TDDFT, especially in terms of coupling to external electromagnetic fields. The gauge invariance of electrodynamics is no longer exactly satisfied when the pseudopotentials introduce non-local potential in Hamiltonian, 136 and how using approximated expressions¹³⁷ impacts the dynamics has not been studied in the context of RT-TDDFT despite its important for studying extended systems.

In addition to recent developments within the RT-TDDFT, coupling electron dynamics to other degrees of freedom is likely to become an important area of future research. Yabana *et al.*

developed a multi-scale Maxwell-TDDFT approach such that the propagation of electromagnetic field is taken into account through a feedback loop between RT-TDDFT and the Maxwell equations.¹ Thus, the electromagnetic field dynamics is explicitly modeled by solving the Maxwell equations with the charge and current densities from RT-TDDFT, and the modified electromagnetic field influences the electron dynamics in turn. Such a description is expected to be important for studying solid-state systems under intense laser fields. 157,158 With the increasingly availability of intense ultrashort laser pulses in experiments, such coupled dynamics has proved highly useful for understanding laser-matter interactions in solids. Other recent developments also extend the description of light-matter interaction by incorporating the quantumelectrodynamics description of light within RT-TDDFT, opening up exciting opportunities into quantum optics and beyond for first-principles theory. 159,160

Together with classical dynamics for the atomic nuclei movement, RT-TDDFT can be readily employed for performing Ehrenfest dynamics as an efficient mixed quantum-classical molecular dynamics approach.⁷⁴ However, such an approach cannot faithfully describe all intricacies of dynamic energy transfer between the electrons and nuclei, and a number of phenomena such as the Joule heating cannot be modeled. 161 Modeling the coupled dynamics of electronic and nuclear motions requires significant future development. Loss of coherence (i.e., decoherence) among the electronic states, due to the nuclei dynamics, is an important aspect, especially for modeling longer-time transition phenomena. The stochastic Schrodinger equation approach¹⁶² could be integrated within the RT-TDDFT conveniently without invoking the density matrix formalism, which is a more natural framework for accounting for the decoherence. Although the computational cost is much higher, the nuclear-electronic orbital formalism has been recently extended to RT-TDDFT such that the nuclei are treated quantummechanically. 131,163 Gross and co-workers also put forward an exact factorization approach to the electron-nuclear wavefunction. 164 The approach has been formally formulated in the context of DFT for electrons and nuclei, 165 and the idea was also used in a recent work to formulate a multi-component RT-TDDFT approach. 166 These exciting developments are expected to open up great opportunities in chemical dynamics such as photochemical reactions in the future.

Despite many outstanding challenges ahead, RT-TDDFT simulations have become a powerful and importantly a practical computational approach over the last few decades. The plane-wave pseudopotential formulation of RT-TDDFT has seen many algorithmic innovations in recent years, enabling us to take advantage of modern HPCs for studying various dynamic phenomena with increasing accuracy in increasingly complex systems. In parallel, new ideas such as spatial decompositions ¹⁶⁷ are also pursued for studying electron dynamics in complex environments. As RT-TDDFT methodologies are developed and used by increasing number of researchers in the quantum chemistry and condensed matter physics communities, many more exciting development and applications are expected in the coming decade.

ACKNOWLEDGMENTS

Y.K. thanks Alfredo Correa and Andre Schleife for the collaborative RT-TDDFT development effort that began at the LLNL.

We thank Erik W. Draeger, Xavier Andrade, and Francois Gygi for helpful discussions on Qbox/Qb@ll code development. This work was financially supported by the National Science Foundation under Award Nos. CHE-1954894 and OAC-17402204. D.C.Y. was supported through an appointment to the Intelligence Community Postdoctoral Research Fellowship Program at Massachusetts Institute of Technology, administered by Oak Ridge Institute for Science and Education through an interagency agreement between the U.S. Department of Energy and the Office of the Director of National Intelligence. We thank the Research Computing at the University of North Carolina at Chapel Hill for computer resources. An award of computer time was also provided by the Innovative and Novel Computational Impact on Theory and Experiment (INCITE) program. This research used resources of the Argonne Leadership Computing Facility (ALCF), which is a DOE Office of Science User Facility supported under Contract No. DE-AC02-06CH11357.

DATA AVAILABILITY

The data that support the findings of this study are available from the corresponding author upon reasonable request.

REFERENCES

- ¹ K. R. S. Devi and S. E. Koonin, "Mean-field approximation to P + He scattering," Phys. Rev. Lett. 47, 27–30 (1981).
- ²H.-D. Meyer, U. Manthe, and L. S. Cederbaum, "The multi-configurational time-dependent Hartree approach," Chem. Phys. Lett. **165**, 73–78 (1990).
- ³X. Li, N. Govind, C. Isborn, A. E. DePrince, and K. Lopata, "Real-time time-dependent electronic structure theory," Chem. Rev. **120**, 9951–9993 (2020).
- ⁴K. Yabana and G. F. Bertsch, "Time-dependent local-density approximation in real time," Phys. Rev. B **54**, 4484–4487 (1996).
- ⁵E. Runge and E. K. U. Gross, "Density-functional theory for time-dependent systems," Phys. Rev. Lett. **52**, 997–1000 (1984).
- ⁶C. A. Ullrich and Z.-h. Yang, "A brief compendium of time-dependent density functional theory," Braz. J. Phys. **44**, 154–188 (2014).
- ⁷C. A. Ullrich, *Time-Dependent Density-Functional Theory: Concepts and Applications* (Oxford Graduate Texts, 2011).
- ⁸M. A. L. Marques and E. K. U. Gross, "Time-dependent density functional theory," Annu. Rev. Phys. Chem. 55, 427–455 (2004).
- ⁹M. Marques, N. Maitra, F. Nogueira, E. K. U. Gross, and A. Rubio, *Fundamentals of Time-Dependent Density Functional Theory* (Springer, 2012), Vol. 837.
- ¹⁰ M. A. L. Marques, C. A. Ullrich, F. Nogueira, A. Rubio, K. Burke, and E. K. U. E. Gross, *Time-Dependent Density Functional Theory* (Springer, Germany, 2006).
- ¹¹M. Casida, "Time-dependent density-functional response theory for molecules," in *Recent Advances in Density Functional Methods, Part I* (World Scientific, Singapore, 1995).
- ¹²M. Petersilka, U. J. Gossmann, and E. K. U. Gross, "Excitation energies from time-dependent density-functional theory," Phys. Rev. Lett. 76, 1212–1215 (1996).
- ¹³B. Walker, A. M. Saitta, R. Gebauer, and S. Baroni, "Efficient approach to time-dependent density-functional perturbation theory for optical spectroscopy," Phys. Rev. Lett. **96**, 113001 (2006).
- ¹⁴M. E. Casida and M. Huix-Rotllant, "Progress in time-dependent density-functional theory," Annu. Rev. Phys. Chem. 63, 287–323 (2012).
- ¹⁵ A. Schleife, E. W. Draeger, Y. Kanai, and A. A. Correa, "Plane-wave pseudopotential implementation of explicit integrators for time-dependent Kohn-Sham equations in large-scale simulations," J. Chem. Phys. **137**, 22A546 (2012).
- ¹⁶A. Schleife, E. W. Draeger, V. M. Anisimov, A. A. Correa, and Y. Kanai, "Quantum dynamics simulation of electrons in materials on high-performance computers," Comput. Sci. Eng. 16, 54 (2014).

- ¹⁷K. Yabana and G. F. Bertsch, "Time-dependent local-density approximation in real time: Application to conjugated molecules," Int. J. Quantum Chem. **75**, 55–66 (1999).
- ¹⁸K. Lopata and N. Govind, "Modeling fast electron dynamics with real-time time-dependent density functional theory: Application to small molecules and chromophores," J. Chem. Theory Comput. 7, 1344–1355 (2011).
- ¹⁹ M. R. Provorse and C. M. Isborn, "Electron dynamics with real-time time-dependent density functional theory," Int. J. Quantum Chem. 116, 739–749 (2016).
- ²⁰J. J. Goings, P. J. Lestrange, and X. Li, "Real-time time-dependent electronic structure theory," Wiley Interdiscip. Rev.: Comput. Mol. Sci. 8, e1341 (2018).
- ²¹ A. Castro, M. A. L. Marques, J. A. Alonso, G. F. Bertsch, and A. Rubio, "Excited states dynamics in time-dependent density functional theory," Eur. Phys. J. D 28, 211–218 (2004).
- ²²W. Liang, C. T. Chapman, and X. Li, "Efficient first-principles electronic dynamics," J. Chem. Phys. 134, 184102 (2011).
- ²⁵G. Wachter, C. Lemell, J. Burgdörfer, S. A. Sato, X.-M. Tong, and K. Yabana, "Ab initio simulation of electrical currents induced by ultrafast laser excitation of dielectric materials," Phys. Rev. Lett. 113, 087401 (2014).
- ²⁴C. Lian, M. Guan, S. Hu, J. Zhang, and S. Meng, "Photoexcitation in solids: First-principles quantum simulations by real-time TDDFT," Adv. Theory Simul. 1, 1800055 (2018).
- ²⁵S. Tussupbayev, N. Govind, K. Lopata, and C. J. Cramer, "Comparison of real-time and linear-response time-dependent density functional theories for molecular chromophores ranging from sparse to high densities of states," J. Chem. Theory Comput. 11, 1102–1109 (2015).
- 26 S. M. Falke *et al.*, "Coherent ultrafast charge transfer in an organic photovoltaic blend," Science 344, 1001 (2014).
- 27 S. Meng and E. Kaxiras, "Electron and hole dynamics in dye-sensitized solar cells: Influencing factors and systematic trends," Nano Lett. 10, 1238–1247 (2010).
 28 R. Hatcher, M. Beck, A. Tackett, and S. T. Pantelides, "Dynamical effects in the interaction of ion beams with solids," Phys. Rev. Lett. 100, 103201 (2008).
- ²⁹D. C. Yost, Y. Yao, and Y. Kanai, "First-principles modeling of electronic stopping in complex matter under ion irradiation," J. Phys. Chem. Lett. 11, 229–237 (2020).
- ³⁰J. M. Pruneda, D. Sánchez-Portal, A. Arnau, J. I. Juaristi, and E. Artacho, "Electronic stopping power in LiF from first principles," Phys. Rev. Lett. 99, 235501 (2007).
- ³¹ A. A. Correa, J. Kohanoff, E. Artacho, D. Sánchez-Portal, and A. Caro, "Nonadiabatic forces in ion-solid interactions: The initial stages of radiation damage," Phys. Rev. Lett. 108, 213201 (2012).
- ³² A. Schleife, Y. Kanai, and A. A. Correa, "Accurate atomistic first-principles calculations of electronic stopping," Phys. Rev. B 91, 014306 (2015).
- ³³D. C. Yost, Y. Yao, and Y. Kanai, "Examining real-time time-dependent density functional theory nonequilibrium simulations for the calculation of electronic stopping power," Phys. Rev. B **96**, 115134 (2017).
- ³⁴Y. Yao, D. C. Yost, and Y. Kanai, "K-shell core-electron excitations in electronic stopping of protons in water from first principles," Phys. Rev. Lett. **123**, 066401 (2019).
- 35 K. G. Reeves, Y. Yao, and Y. Kanai, "Electronic stopping power in liquid water for protons and α particles from first principles," Phys. Rev. B **94**, 041108 (2016).
- 36 D. C. Yost and Y. Kanai, "Electronic stopping for protons and α particles from first-principles electron dynamics: The case of silicon carbide," Phys. Rev. B **94**, 115107 (2016).
- 37 D. C. Yost and Y. Kanai, "Electronic excitation dynamics in DNA under proton and α-particle irradiation," J. Am. Chem. Soc. 141, 5241–5251 (2019).
- ³⁸Z. Wang, S.-S. Li, and L.-W. Wang, "Efficient real-time time-dependent density functional theory method and its application to a collision of an ion with a 2D material," Phys. Rev. Lett. 114, 063004 (2015).
- ³⁹R. D. Senanayake, D. B. Lingerfelt, G. U. Kuda-Singappulige, X. Li, and C. M. Aikens, "Real-time TDDFT investigation of optical absorption in gold nanowires," J. Phys. Chem. C **123**, 14734–14745 (2019).
- ⁴⁰M. A. L. Marques, X. López, D. Varsano, A. Castro, and A. Rubio, "Time-dependent density-functional approach for biological chromophores: The case of the green fluorescent protein," Phys. Rev. Lett. 90, 258101 (2003).

- ⁴¹ M. Schultze *et al.*, "Attosecond band-gap dynamics in silicon," Science **346**, 1348 (2014).
- ⁴²K. Lopata, B. E. Van Kuiken, M. Khalil, and N. Govind, "Linear-response and real-time time-dependent density functional theory studies of core-level near-edge x-ray absorption," J. Chem. Theory Comput. **8**, 3284–3292 (2012).
- ⁴³C. D. Pemmaraju, F. D. Vila, J. J. Kas, S. A. Sato, J. J. Rehr, K. Yabana, and D. Prendergast, "Velocity-gauge real-time TDDFT within a numerical atomic orbital basis set," Comput. Phys. Commun. 226, 30–38 (2018).
- ⁴⁴A. R. Attar, A. Bhattacherjee, C. D. Pemmaraju, K. Schnorr, K. D. Closser, D. Prendergast, and S. R. Leone, "Femtosecond x-ray spectroscopy of an electrocyclic ring-opening reaction," Science **356**, 54 (2017).
- ⁴⁵C. D. Pemmaraju, "Valence and core excitons in solids from velocity-gauge real-time TDDFT with range-separated hybrid functionals: An LCAO approach," Comput. Condens. Matter 18, e00348 (2019).
- ⁴⁶J. J. Goings and X. Li, "An atomic orbital based real-time time-dependent density functional theory for computing electronic circular dichroism band spectra," J. Chem. Phys. **144**, 234102 (2016).
- ⁴⁷B. Peng, D. B. Lingerfelt, F. Ding, C. M. Aikens, and X. Li, "Real-time TDDFT studies of exciton decay and transfer in silver nanowire arrays," J. Phys. Chem. C 119, 6421–6427 (2015).
- ⁴⁸J. Ma, Z. Wang, and L.-W. Wang, "Interplay between plasmon and single-particle excitations in a metal nanocluster," Nat. Commun. 6, 10107 (2015).
 ⁴⁹C. L. Moss, C. M. Isborn, and X. Li, "Ehrenfest dynamics with a time-dependent
- ⁴⁹C. L. Moss, C. M. Isborn, and X. Li, "Ehrenfest dynamics with a time-dependent density-functional-theory calculation of lifetimes and resonant widths of charge-transfer states of Li⁺ near an aluminum cluster surface," Phys. Rev. A **80**, 024503 (2009).
- ⁵⁰C. M. Isborn, X. Li, and J. C. Tully, "Time-dependent density functional theory Ehrenfest dynamics: Collisions between atomic oxygen and graphite clusters," J. Chem. Phys. **126**, 134307 (2007).
- ⁵¹M. S. Mrudul, N. Tancogne-Dejean, A. Rubio, and G. Dixit, "High-harmonic generation from spin-polarised defects in solids," npj Comput. Mater. **6**, 10 (2020).
- ⁵²N. Tancogne-Dejean, O. D. Mücke, F. X. Kärtner, and A. Rubio, "Impact of the electronic band structure in high-harmonic generation spectra of solids," Phys. Rev. Lett. **118**, 087403 (2017).
- ⁵³Y. Miyamoto, H. Zhang, X. Cheng, and A. Rubio, "Modeling of laser-pulse induced water decomposition on two-dimensional materials by simulations based on time-dependent density functional theory," Phys. Rev. B **96**, 115451 (2017).
- ⁵⁴D. C. Yost, Y. Yao, and Y. Kanai, "Propagation of maximally localized Wannier functions in real-time TDDFT," J. Chem. Phys. 150, 194113 (2019).
- ⁵⁵H. Hübener, M. A. Sentef, U. De Giovannini, A. F. Kemper, and A. Rubio, "Creating stable Floquet–Weyl semimetals by laser-driving of 3D Dirac materials," Nat. Commun. 8, 13940–13948 (2017).
- ⁵⁶D. Shin, S. A. Sato, H. Hübener, U. De Giovannini, J. Kim, N. Park, and A. Rubio, "Unraveling materials Berry curvature and Chern numbers from real-time evolution of Bloch states," Proc. Natl. Acad. Sci. U. S. A. 116, 4135 (2019).
- ⁵⁷R. Zhou, D. C. Yost, and Y. Kanai, "First-principles demonstration of nonadiabatic thouless pumping of electrons in a molecular system," J. Phys. Chem. Lett. 12, 4496–4503 (2021).
- ⁵⁸ M. Valiev *et al.*, "NWChem: A comprehensive and scalable open-source solution for large scale molecular simulations," Comput. Phys. Commun. 181, 1477–1489 (2010).
- ⁵⁹Y. Takimoto, F. D. Vila, and J. J. Rehr, "Real-time time-dependent density functional theory approach for frequency-dependent nonlinear optical response in photonic molecules," J. Chem. Phys. 127, 154114 (2007).
- 60 J. M. Soler, E. Artacho, J. D. Gale, A. García, J. Junquera, P. Ordejón, and D. Sánchez-Portal, "The SIESTA method for *ab initio* order-N materials simulation," J. Phys.: Condens. Matter 14, 2745–2779 (2002).
- 61 T. Kunert and R. Schmidt, "Non-adiabatic quantum molecular dynamics: General formalism and case study ${\rm H_2}^+$ in strong laser fields," Eur. Phys. J. D **25**, 15–24 (2003)
- ⁶²T. D. Kühne *et al.*, "CP2K: An electronic structure and molecular dynamics software package—Quickstep: Efficient and accurate electronic structure calculations," J. Chem. Phys. **152**, 194103 (2020).

- ⁶³ M. Noda *et al.*, "SALMON: Scalable ab-initio light–matter simulator for optics and nanoscience," Comput. Phys. Commun. 235, 356–365 (2019).
- ⁶⁴M. A. L. Marques, A. Castro, G. F. Bertsch, and A. Rubio, "Octopus: A first-principles tool for excited electron-ion dynamics," Comput. Phys. Commun. **151**, 60–78 (2003).
- ⁶⁵N. Tancogne-Dejean *et al.*, "Octopus, a computational framework for exploring light-driven phenomena and quantum dynamics in extended and finite systems," J. Chem. Phys. **152**, 124119 (2020).
- ⁶⁶T. S. Nguyen and J. Parkhill, "Nonadiabatic dynamics for electrons at secondorder: Real-time TDDFT and OSCF₂," J. Chem. Theory Comput. **11**, 2918–2924 (2015).
- ⁶⁷Y. Zhu and J. M. Herbert, "Self-consistent predictor/corrector algorithms for stable and efficient integration of the time-dependent Kohn-Sham equation," J. Chem. Phys. **148**, 044117 (2018).
- ⁶⁸Y. Shao *et al.*, "Advances in molecular quantum chemistry contained in the Q-Chem 4 program package," Mol. Phys. **113**, 184–215 (2015).
- ⁶⁹ X. Li, S. M. Smith, A. N. Markevitch, D. A. Romanov, R. J. Levis, and H. B. Schlegel, "A time-dependent Hartree-Fock approach for studying the electronic optical response of molecules in intense fields," Phys. Chem. Chem. Phys. 7, 233–239 (2005).
- ⁷⁰ I. Maliyov, J.-P. Crocombette, and F. Bruneval, "Electronic stopping power from time-dependent density-functional theory in Gaussian basis," Eur. Phys. J. B 91, 172 (2018).
- ⁷¹F. Bruneval, T. Rangel, S. M. Hamed, M. Shao, C. Yang, and J. B. Neaton, "MOLGW 1: Many-body perturbation theory software for atoms, molecules, and clusters," Comput. Phys. Commun. 208, 149–161 (2016).
- ⁷²F. Gygi, "Architecture of Qbox: A scalable first-principles molecular dynamics code," IBM J. Res. Dev. **52**, 137–144 (2008).
- 73 E. W. Draeger and F. Gygi, Qbox Code, Qb@Ll Version, Lawrence Livermore National Laboratory.
- ⁷⁴ X. Li, J. C. Tully, H. B. Schlegel, and M. J. Frisch, "Ab initio Ehrenfest dynamics," J. Chem. Phys. **123**, 084106–084107 (2005).
- ⁷⁵ M. C. Payne, M. P. Teter, D. C. Allan, T. A. Arias, and J. D. Joannopoulos, "Iterative minimization techniques for ab initio total-energy calculations: Molecular dynamics and conjugate gradients," Rev. Mod. Phys. **64**, 1045–1097 (1992)
- ⁷⁶ M. Fuchs and M. Scheffler, "Ab initio pseudopotentials for electronic structure calculations of poly-atomic systems using density-functional theory," Comput. Phys. Commun. 119, 67–98 (1999).
- ⁷⁷D. Marx and J. Hutter, Ab Initio Molecular Dynamics: Basic Theory and Advanced Methods (Cambridge University Press, Cambridge, 2009).
- ⁷⁸X. Andrade *et al.*, "Real-space grids and the Octopus code as tools for the development of new simulation approaches for electronic systems," Phys. Chem. Chem. Phys. **17**, 31371–31396 (2015).
- ⁷⁹V. Heine, "The pseudopotential concept," in *Solid State Physics*, edited by H. Ehrenreich, F. Seitz, and D. Turnbull (Academic Press, 1970), Vol. 24, pp. 1–36.
- ⁸⁰D. R. Hamann, M. Schlüter, and C. Chiang, "Norm-conserving pseudopotentials," Phys. Rev. Lett. 43, 1494–1497 (1979).
- ⁸¹L. Kleinman and D. M. Bylander, "Efficacious form for model pseudopotentials," Phys. Rev. Lett. **48**, 1425–1428 (1982).
- ⁸²M. J. van Setten, M. Giantomassi, E. Bousquet, M. J. Verstraete, D. R. Hamann, X. Gonze, and G.-M. Rignanese, "The PseudoDojo: Training and grading a 85 element optimized norm-conserving pseudopotential table," Comput. Phys. Commun. 226, 39–54 (2018).
- ⁸³ P. E. Blöchl, "Projector augmented-wave method," Phys. Rev. B 50, 17953–17979 (1994).
- ⁸⁴ A. Ojanperä, V. Havu, L. Lehtovaara, and M. Puska, "Nonadiabatic Ehrenfest molecular dynamics within the projector augmented-wave method," J. Chem. Phys. 136, 144103–144109 (2012).
- 85 O. Sugino and Y. Miyamoto, "Density-functional approach to electron dynamics: Stable simulation under a self-consistent field," Phys. Rev. B 59, 2579–2586 (1999).
- ⁸⁶Y. Miyamoto, O. Sugino, and Y. Mochizuki, "Real-time electron-ion dynamics for photoinduced reactivation of hydrogen-passivated donors in gaas," Appl. Phys. Lett. 75, 2915–2917 (1999).

- ⁸⁷N. T. Maitra and K. Burke, "On the Floquet formulation of time-dependent density functional theory," Chem. Phys. Lett. **359**, 237–240 (2002).
- ⁸⁸ A. Castro, M. A. L. Marques, and A. Rubio, "Propagators for the time-dependent Kohn–Sham equations," J. Chem. Phys. **121**, 3425–3433 (2004).
- ⁸⁹ A. Gómez Pueyo, M. A. L. Marques, A. Rubio, and A. Castro, "Propagators for the time-dependent Kohn–Sham equations: Multistep, Runge–Kutta, exponential Runge–Kutta, and commutator free Magnus methods," J. Chem. Theory Comput. 14, 3040–3052 (2018).
- ⁹⁰D. A. Rehn, Y. Shen, M. E. Buchholz, M. Dubey, R. Namburu, and E. J. Reed, "ODE integration schemes for plane-wave real-time time-dependent density functional theory," J. Chem. Phys. 150, 014101 (2019).
- ⁹¹Y. Li, S. He, A. Russakoff, and K. Varga, "Accurate time propagation method for the coupled Maxwell and Kohn-Sham equations," Phys. Rev. E **94**, 023314 (2016).
- ⁹²X. Qian, J. Li, X. Lin, and S. Yip, "Time-dependent density functional theory with ultrasoft pseudopotentials: Real-time electron propagation across a molecular junction," Phys. Rev. B **73**, 035408 (2006).
- ⁹³E. W. Draeger, X. Andrade, J. A. Gunnels, A. Bhatele, A. Schleife, and A. A. Correa, "Massively parallel first-principles simulation of electron dynamics in materials," J. Parallel Distrib. Comput. 106, 205–214 (2017).
- ⁹⁴N. T. Maitra, "Perspective: Fundamental aspects of time-dependent density functional theory," J. Chem. Phys. **144**, 220901 (2016).
- ⁹⁵G. Vignale and W. Kohn, "Current-dependent exchange-correlation potential for dynamical linear response theory," Phys. Rev. Lett. 77, 2037–2040 (1996).
- ⁹⁶H. O. Wijewardane and C. A. Ullrich, "Time-dependent Kohn-Sham theory with memory," Phys. Rev. Lett. 95, 086401 (2005).
- ⁹⁷C. A. Ullrich and I. V. Tokatly, "Nonadiabatic electron dynamics in time-dependent density-functional theory," Phys. Rev. B 73, 235102 (2006).
- ⁹⁸C. A. Ullrich, "Time-dependent density-functional theory beyond the adiabatic approximation: Insights from a two-electron model system," J. Chem. Phys. **125**, 234108 (2006).
- ⁹⁹J. M. Escartín, M. Vincendon, P. Romaniello, P. M. Dinh, P.-G. Reinhard, and E. Suraud, "Towards time-dependent current-density-functional theory in the non-linear regime," J. Chem. Phys. **142**, 084118 (2015).
- 100 R. van Leeuwen, "Mapping from densities to potentials in time-dependent density-functional theory," Phys. Rev. Lett. 82, 3863–3866 (1999).
- ¹⁰¹N. T. Maitra, K. Burke, and C. Woodward, "Memory in time-dependent density functional theory," Phys. Rev. Lett. 89, 023002 (2002).
- ¹⁰²J. I. Fuks and N. T. Maitra, "Challenging adiabatic time-dependent density functional theory with a Hubbard dimer: The case of time-resolved long-range charge transfer," Phys. Chem. Chem. Phys. 16, 14504–14513 (2014).
- ¹⁰³J. I. Fuks, N. Helbig, I. V. Tokatly, and A. Rubio, "Nonlinear phenomena in time-dependent density-functional theory: What Rabi oscillations can teach us," Phys. Rev. B 84, 075107 (2011).
- ¹⁰⁴J. I. Fuks, L. Lacombe, S. E. B. Nielsen, and N. T. Maitra, "Exploring non-adiabatic approximations to the exchange-correlation functional of TDDFT," Phys. Chem. Chem. Phys. 20, 26145–26160 (2018).
- 105 Y. Suzuki, R. Nagai, and J. Haruyama, "Machine learning exchange-correlation potential in time-dependent density-functional theory," Phys. Rev. A 101, 050501 (2020).
- ¹⁰⁶R. Nagai, R. Akashi, S. Sasaki, and S. Tsuneyuki, "Neural-network Kohn-Sham exchange-correlation potential and its out-of-training transferability," J. Chem. Phys. 148, 241737 (2018).
- 107Y. Kanai, X. Wang, A. Selloni, and R. Car, "Testing the TPSS meta-generalized-gradient-approximation exchange-correlation functional in calculations of transition states and reaction barriers," J. Chem. Phys. 125, 234104–234108 (2006)
- 108 Y. Yao and Y. Kanai, "Plane-wave pseudopotential implementation and performance of scan meta-GGA exchange-correlation functional for extended systems," J. Chem. Phys. 146, 224105 (2017).
- 109 X. Wu, A. Selloni, and R. Car, "Order-N implementation of exact exchange in extended insulating systems," Phys. Rev. B 79, 085102 (2009).

- ¹¹⁰W. Dawson and F. Gygi, "Performance and accuracy of recursive subspace bisection for hybrid DFT calculations in inhomogeneous systems," J. Chem. Theory Comput. 11, 4655–4663 (2015).
- 111 P. Broqvist, A. Alkauskas, and A. Pasquarello, "Hybrid-functional calculations with plane-wave basis sets: Effect of singularity correction on total energies, energy eigenvalues, and defect energy levels," Phys. Rev. B 80, 085114 (2009).
- 112I. Carnimeo, S. Baroni, and P. Giannozzi, "Fast hybrid density-functional computations using plane-wave basis sets," Electron. Struct. 1, 015009 (2019).
- ¹¹³I. Duchemin and F. Gygi, "A scalable and accurate algorithm for the computation of Hartree-Fock exchange," Comput. Phys. Commun. **181**, 855–860 (2010).
- ¹¹⁴L. Lin, "Adaptively compressed exchange operator," J. Chem. Theory Comput. 12, 2242–2249 (2016).
- 115 F. Gygi and I. Duchemin, "Efficient computation of Hartree-Fock exchange using recursive subspace bisection," J. Chem. Theory Comput. 9, 582–587 (2013).
 116 F. Gygi, "Compact representations of Kohn-Sham invariant subspaces," Phys. Rev. Lett. 102, 166406 (2009).
- 117W. Jia and L. Lin, "Fast real-time time-dependent hybrid functional calculations with the parallel transport gauge and the adaptively compressed exchange formulation," Comput. Phys. Commun. 240, 21–29 (2019).
- ¹¹⁸W. Jia, D. An, L.-W. Wang, and L. Lin, "Fast real-time time-dependent density functional theory calculations with the parallel transport gauge," J. Chem. Theory Comput. 14, 5645–5652 (2018).
- ¹¹⁹T. Aschebrock and S. Kümmel, "Ultranonlocality and accurate band gaps from a meta-generalized gradient approximation," Phys. Rev. Res. **1**, 033082 (2019).
- ¹²⁰N. T. Maitra, "Charge transfer in time-dependent density functional theory," J. Phys.: Condens. Matter 29, 423001 (2017).
- ¹²¹N. Marzari and D. Vanderbilt, "Maximally localized generalized Wannier functions for composite energy bands," Phys. Rev. B **56**, 12847–12865 (1997).
- ¹²²W. Kohn, "Density functional and density matrix method scaling linearly with the number of atoms," Phys. Rev. Lett. **76**, 3168–3171 (1996).
- 123 E. Prodan and W. Kohn, "Nearsightedness of electronic matter," Proc. Natl. Acad. Sci. U. S. A. 102, 11635 (2005).
- ¹²⁴N. Marzari, A. A. Mostofi, J. R. Yates, I. Souza, and D. Vanderbilt, "Maximally localized Wannier functions: Theory and applications," Rev. Mod. Phys. 84, 1419–1475 (2012).
- ¹²⁵H.-Y. Ko, J. Jia, B. Santra, X. Wu, R. Car, and R. A. DiStasio Jr, "Enabling large-scale condensed-phase hybrid density functional theory based *ab initio* molecular dynamics. 1. Theory, algorithm, and performance," J. Chem. Theory Comput. 2020, 16, 3757–3785.
- ¹²⁶M. Sharma, Y. Wu, and R. Car, "Ab initio molecular dynamics with maximally localized Wannier functions," Int. J. Quantum Chem. 95, 821–829 (2003).
- 127 J. W. Thomas, R. Iftimie, and M. E. Tuckerman, "Field theoretic approach to dynamical orbital localization in ab initio molecular dynamics," Phys. Rev. B 69, 125105 (2004).
- 128J. P. Perdew, K. Burke, and M. Ernzerhof, "Generalized gradient approximation made simple," Phys. Rev. Lett. 77, 3865–3868 (1996).
- 129 J. P. Perdew, M. Ernzerhof, and K. Burke, "Rationale for mixing exact exchange with density functional approximations," J. Chem. Phys. 105, 9982–9985 (1996).
- ¹³⁰D. Vanderbilt, "Optimally smooth norm-conserving pseudopotentials," Phys. Rev. B 32, 8412–8415 (1985).
- 131 R. Zhou and Y. Kanai, "Dynamical transition orbitals: A particle-hole description in real-time TDDFT dynamics," J. Chem. Phys. 154, 054107 (2021).
- $^{132}\mathrm{R}.$ L. Martin, "Natural transition orbitals," J. Chem. Phys. 118, 4775–4777 (2003).
- ¹³³N. T. Maitra, I. Souza, and K. Burke, "Current-density functional theory of the response of solids." Phys. Rev. B **68**: 045109 (2003).
- response of solids," Phys. Rev. B **68**, 045109 (2003).

 134P. Umari and A. Pasquarello, "Ab initio molecular dynamics in a finite homogeneous electric field," Phys. Rev. Lett. **89**, 157602 (2002).
- ¹³⁵M. Sharma, R. Resta, and R. Car, "Intermolecular dynamical charge fluctuations in water: A signature of the H-bond network," Phys. Rev. Lett. 95, 187401 (2005).
- ¹³⁶A. F. Starace, "Length and velocity formulas in approximate oscillator-strength calculations," Phys. Rev. A 3, 1242–1245 (1971).

- 137 S. Ismail-Beigi, E. K. Chang, and S. G. Louie, "Coupling of nonlocal potentials to electromagnetic fields," Phys. Rev. Lett. 87, 087402 (2001).
- 138 Francois Gygi began the Qbox code development for performing large-scale FPMD simulations at the Lawrence Livermore National Laboratory (LLNL). The development effort has continued separately under the name of Qb@ll (coined from "Qbox at Livermore Laboratory") at the LLNL even after Gygi's move to University of California at Davis relocated the main Qbox development effort. Our RT-TDDFT development started in 2010 at the LLNL, and the development has since continued collaboratively with former LLNL scientists who moved to academia, including Yosuke Kanai (University of North Carolina at Chapel Hill) and Andre Schleife (University of Illinois at Urbana Champaign). The Qb@ll effort at the LLNL is currently led mainly by Erik W. Draeger, Alfredo Correa, and Xavier Andrade.
- 139 X. Andrade, A. Castro, D. Zueco, J. L. Alonso, P. Echenique, F. Falceto, and Á. Rubio, "Modified Ehrenfest formalism for efficient large-scale ab initio molecular dynamics," J. Chem. Theory Comput. 5, 728–742 (2009).
- ¹⁴⁰X. Andrade, A. A. Correa, and T. Ogitsu, private communication (2021).
- ¹⁴¹W. F. Chan, G. Cooper, and C. E. Brion, "The electronic spectrum of water in the discrete and continuum regions. Absolute optical oscillator strengths for photoabsorption (6–200 eV)," Chem. Phys. 178, 387–400 (1993).
- ¹⁴²D. R. Mason, J. le Page, C. P. Race, W. M. C. Foulkes, M. W. Finnis, and A. P. Sutton, "Electronic damping of atomic dynamics in irradiation damage of metals," J. Phys.: Condens. Matter 19, 436209 (2007).
- ¹⁴³N. D. Drummond, Z. Radnai, J. R. Trail, M. D. Towler, and R. J. Needs, "Diffusion quantum Monte Carlo study of three-dimensional Wigner crystals," Phys. Rev. B 69, 085116 (2004).
- ¹⁴⁴J. P. Perdew and K. Schmidt, "Jacob's ladder of density functional approximations for the exchange-correlation energy," AIP Conf. Proc. 577, 1–20 (2001).
- ¹⁴⁵R. Car, "Fixing Jacob's ladder," Nat. Chem. **8**, 820–821 (2016).
- ¹⁴⁶J. Sun, A. Ruzsinszky, and J. P. Perdew, "Strongly constrained and appropriately normed semilocal density functional," Phys. Rev. Lett. 115, 036402 (2015).
- ¹⁴⁷J. F. Ziegler, M. D. Ziegler, and J. P. Biersack, "SRIM—The stopping and range of ions in matter," Nucl. Instrum. Methods Phys. Res., Sect. B 268, 1818–1823 (2010).
- ¹⁴⁸D. Vanderbilt, Berry Phases in Electronic Structure Theory: Electric Polarization, Orbital Magnetization and Topological Insulators (Cambridge University Press, Cambridge, 2018).
- $^{149}\rm{R}.$ Resta and D. Vanderbilt, "Theory of polarization: A modern approach," in *Physics of Ferroelectrics: A Modern Perspective* (Springer Berlin Heidelberg, Berlin, Heidelberg, 2007), pp. 31–68.
- ¹⁵⁰D. J. Thouless, "Quantization of particle transport," Phys. Rev. B 27, 6083–6087 (1983).
- ¹⁵¹S. Nakajima, T. Tomita, S. Taie, T. Ichinose, H. Ozawa, L. Wang, M. Troyer, and Y. Takahashi, "Topological Thouless pumping of ultracold fermions," Nat. Phys. 12, 296–300 (2016).
- ¹⁵²M. Lohse, C. Schweizer, O. Zilberberg, M. Aidelsburger, and I. Bloch, "A Thouless quantum pump with ultracold bosonic atoms in an optical superlattice," Nat. Phys. 12, 350–354 (2016).
- 153 Y. Kuno, "Non-adiabatic extension of the Zak phase and charge pumping in the Rice–Mele model," Eur. Phys. J. B **92**, 195 (2019).
- ¹⁵⁴M. Repisky, L. Konecny, M. Kadek, S. Komorovsky, O. L. Malkin, V. G. Malkin, and K. Ruud, "Excitation energies from real-time propagation of the four-component Dirac-Kohn-Sham equation," J. Chem. Theory Comput. 11, 980–991 (2015).
- ¹⁵⁵J. J. Goings, J. M. Kasper, F. Egidi, S. Sun, and X. Li, "Real time propagation of the exact two component time-dependent density functional theory," J. Chem. Phys. 145, 104107 (2016).
- ¹⁵⁶K. Yabana, T. Sugiyama, Y. Shinohara, T. Otobe, and G. F. Bertsch, "Time-dependent density functional theory for strong electromagnetic fields in crystalline solids," Phys. Rev. B **85**, 045134 (2012).
- 157S. A. Sato and K. Yabana, "Maxwell + TDDFT multi-scale simulation for laser-matter interactions," J. Adv. Simul. Sci. Eng. 1, 98–110 (2014).
- ¹⁵⁸C. Covington, D. Kidd, H. Buckner, H. Appel, and K. Varga, "Time propagation of the coupled Maxwell and Kohn-Sham equations using the Riemann-Silberstein formalism," Phys. Rev. E 100, 053301 (2019).

Rev. B 93, 024306 (2016).

- ¹⁵⁹I. V. Tokatly, "Time-dependent density functional theory for many-electron systems interacting with cavity photons," Phys. Rev. Lett. 110, 233001 (2013).
- 160 J. Flick, M. Ruggenthaler, H. Appel, and A. Rubio, "Kohn–Sham approach to quantum electrodynamical density-functional theory: Exact time-dependent effective potentials in real space," Proc. Natl. Acad. Sci. U. S. A. 112, 15285 (2015).
 161 V. Rizzi, T. N. Todorov, J. J. Kohanoff, and A. A. Correa, "Electron-phonon thermalization in a scalable method for real-time quantum dynamics," Phys.

¹⁶²O. V. Prezhdo, "Mean field approximation for the stochastic Schrödinger equation," J. Chem. Phys. 111, 8366–8377 (1999).

- ¹⁶³L. Zhao, Z. Tao, F. Pavošević, A. Wildman, S. Hammes-Schiffer, and X. Li, "Real-time time-dependent nuclear-electronic orbital approach: Dynamics
- beyond the Born-Oppenheimer approximation," J. Phys. Chem. Lett. 11, 4052-4058 (2020).
- 164 A. Abedi, N. T. Maitra, and E. K. U. Gross, "Exact factorization of the time-dependent electron-nuclear wave function," Phys. Rev. Lett. 105, 123002 (2010).
- ¹⁶⁵R. Requist and E. K. U. Gross, "Exact factorization-based density functional theory of electrons and nuclei," Phys. Rev. Lett. 117, 193001 (2016).
- ¹⁶⁶Y. Suzuki, S. Hagiwara, and K. Watanabe, "Time-dependent multicomponent density functional theory for coupled electron-positron dynamics," Phys. Rev. Lett. **121**, 133001 (2018).
- ¹⁶⁷A. Krishtal, D. Ceresoli, and M. Pavanello, "Subsystem real-time time dependent density functional theory," J. Chem. Phys. 142, 154116 (2015).